Journal of Hazardous Materials 405 (2021) 124230

Contents lists available at ScienceDirect

Journal of Hazardous Materials

journal homepage: www.elsevier.com/locate/jhazmat

Research paper

Identification of potential toxicants in sediments from an industrialized area in Pohang, South Korea: Application of a cell viability assay of microalgae using flow cytometry

Seong-Ah An [a], Seongjin Hong [a,*], Junghyun Lee [b], Jihyun Cha [a], Sunggyu Lee [c], Hyo-Bang Moon [c], John P. Giesy [d,e], Jong Seong Khim [b,*]

[a] Department of Ocean Environmental Sciences, Chungnam National University, Daejeon 34134, Republic of Korea
[b] School of Earth and Environmental Sciences & Research Institute of Oceanography, Seoul National University, Seoul 08826, Republic of Korea
[c] Department of Marine Science and Convergence Engineering, Hanyang University, Ansan 15588, Republic of Korea
[d] Department of Veterinary Biomedical Sciences & Toxicology Centre, University of Saskatchewan, Saskatoon, Saskatchewan S7N5B3, Canada
[e] Department of Environmental Sciences, Baylor University, Waco, Texas 76706, United States

ARTICLE INFO

Keywords:
Effect-directed analysis
PAHs
Sediment
GC-QTOFMS
Toxicity
Industrial complex

ABSTRACT

Potential toxicants in sediments collected from an industrialized bay of Korea were identified by use of effect-directed analysis (EDA). Three marine microalgal bioassays (*Dunaliella tertiolecta*, *Isochrysis galbana*, and *Phaeodactylum tricornutum*) with diverse endpoints were employed. Initial screening of raw organic extracts of sediments indicated large variations among locations and species in a traditional endpoint "inhibition of growth". After fractionation, inhibition of growths increased significantly, particularly in some fractions containing aromatics with log K_{OW} 5–6 (F2.6). While viabilities of cells were adversely affected in more fractions, including F2.6–F2.7 (log K_{OW} 5–7) and F3.5–F3.6 (log K_{OW} 4–6). Among the several endpoints of viability, esterase activity seemed to be more sensitive, followed by integrity of cell membranes, chlorophyll *a*, cell size, and intracellular complexity. Instrumental analyses indicated that toxicities to microalgae observed in F2.7 could not be fully explained by target PAHs. Full-scan screening analysis using GC-QTOFMS identified 58 compounds in F2.7 with matching scores ≥90%. Based on toxic potencies for these compounds predicted by ECOSAR, several causative agents, including 1-phenylpyrene, dibenz[*a*,*c*]anthracene, and picene were suggested. Overall, viability of microalgae provided sensitive and high-resolution toxicity screening of samples into integrative assessment of sediment.

1. Introduction

In coastal environments, hydrophobic chemicals tend to accumulate in sediments and persist for extended periods, potentially affecting organisms directly and indirectly (Power et al., 1991; Grote et al., 2005; Brack et al., 2009). Assessment of pollution of sediments, using instrumental analyses, such as targeted analysis, is limited due to complexities of environmental samples, which can contain thousands of chemicals (Brack, 2003). Bioassays can integrate effects of known and unidentified toxic substances; however, it is difficult to identify the causative chemicals (Brack, 2003). Effect-directed analysis (EDA), which combines bioassays, fractionation, and instrumental analysis, is a powerful tool for identifying key toxicants in environmental samples by reducing complexity through iterative fractionations (Brack, 2003; Lee et al., 2020).

Because of their sensitivity and ability to test large numbers of samples quickly, in vitro bioassays are primarily used in EDA (Brack et al., 2016). However, in vitro bioassays are limited in their ability to assess overall effects on relevant organisms; consequently, demand for in vivo assays for use in EDA studies is increasing (Brack et al., 2016; Guo et al., 2019). In vivo bioassays have the advantage of using more environmentally relevant evaluations and assess diverse biological endpoints after a single exposure. Because microalgae are primary producers with major contributions to aquatic ecosystems, they are widely used to assess toxic potencies of extracts of environmental matrices (Burkiewicz et al., 2005; Prado et al., 2011; Booij et al., 2014).

* Corresponding authors.
E-mail addresses: hongseongjin@cnu.ac.kr (S. Hong), jskocean@snu.ac.kr (J.S. Khim).

https://doi.org/10.1016/j.jhazmat.2020.124230
Received 8 August 2020; Received in revised form 27 September 2020; Accepted 7 October 2020
Available online 10 October 2020

In addition, microalgal bioassays have shown advantages, such as culture flexibility, rapid growth potential, and sensitive responsiveness (Radix et al., 2000; Prato et al., 2012; Emelogu et al., 2014).

Several previous studies successfully demonstrated some new environmental toxicants by utilizing the EDA approach with in vivo bioassays of microalgae. For examples, triclosan, N-phenyl-2-naphthylamine, and 7 H-benzo[*de*]anthracen-7-one were newly identified environmental toxicants based on inhibition of growth (Bandow et al., 2009; Schwab et al., 2009). In particular, triclosan, which has been banned in the United States (United States Food and Drug Administration USFDA, 2016), was identified as a major inhibitor of microalgal growth (Brack et al., 2009). However, those previous studies focused mainly on inhibition of growth as measured by cell division, during EDA (Brack et al., 2016; Bergmann et al., 2017). Studies on inhibition of growth of microalgae require relatively larger toxic potency; consequently, it is not desirable for use in EDA of environmental samples, particularly when testing their numerous fractions during EDA (Tang et al., 2013; Brack et al., 2016). In addition, detailed information on adverse outcome pathways (AOPs) that result in inhibition of microalgae remains limited.

Assays of viability of microalgal cells, using flow cytometry, can provide measurements of sensitive physiological responses of individual cells (Funahashi and Hanna, 1997; Franqueira et al., 2000; Prado et al., 2011). Of note, the endpoint has a statistical advantage as it can easily measure enough number of samples, viz., >10,000 cells in a single measurement (Baldetorp et al., 1989; Eudey, 1996). Determination of viabilities of cells by use of flow cytometry involves evaluation of individual cells for various parameters, including size, intracellular complexity, chlorophyll *a* autofluorescence (Chl. *a*), esterase activity, membrane damage, mitochondrial membrane potential, contents of reactive oxygen species, etc. (Prado et al., 2011, 2012; Almeida et al., 2019; Dupraz et al., 2019; Machado and Soares, 2019). Parameters of viability of cells provide early warning of sub-lethal effects on microalgae. Microalgae that have lost their cellular health due to stresses by toxic substances become difficult to perform their original functions in the marine ecosystem, such as primary production (Béchet et al., 2017). Our recent study identified microalgal toxicants in contaminated sediments using a cell viability assay with various endpoints, highlighting significant cell membrane damage being detected at lesser concentrations compared to the EC50 for inhibition of growth (Lee et al., 2020). Thus, cell viability assays could be a promising tool for the EDA usage to improve standard microalgal bioassays, and elucidate modes of toxic action to microalgae during EDA. Of note, however, special caution is required for cell viability assay using a flow cytometry technique in that cells need to be solitary living and of fairly uniform size and shape.

In recent years, during EDA studies, full-scan screening (nontarget) analysis (FSA) has been successfully applied to identify previously untargeted toxicants in more potent fractions of environmental samples (Gómez et al., 2009; Booij et al., 2014). Low-resolution mass spectrometry has limited capacity to measure the accurate mass of untargeted compounds, or to distinguish compounds of similar *m/z* among complex mixtures. Thus, instrumental analysis using ultrahigh-resolution mass spectrometry (UHRMS), such as time-of-flight mass spectrometry (TOFMS) and Orbitrap mass spectrometry, is increasingly utilized for FSA (Hernández et al., 2012; Hollender et al., 2018; Cha et al., 2019; Lee et al., 2020). A previous study identified PSII stressors, such as irgarol, diuron, and terbuthylazine in surface water by use of LC-TOFMS (Booij et al., 2014).

Pohang City, South Korea, which borders Yeongil Bay, supports national industrial complexes and has more than half a million residents. Various pollutants originate from the industrial complexes, with approximately 290,000 tons of treated sewage effluent being discharged daily into Yeongil Bay. Several previous studies detected polycyclic aromatic hydrocarbons (PAHs) and alkylphenols (APs) in sediments of Pohang and/or Yeongil Bay regions of which concentrations exceeded the Interim Sediment Quality Guidelines (ISQG) suggested by the Canadian Council of Ministers of the Environment (CCME) (Koh et al., 2004, 2006; Kim et al., 2014). Styrene oligomers (SOs), which are emerging pollutants, have been reported to distributed in industrial areas of South Korea, but had not been investigated in Yeongil Bay (Hong et al., 2016; Cha et al., 2019; Kim et al., 2019).

The objectives of the present study were to assess toxic potencies of persistent toxic substances (PTSs) in sediments to microalgae and identify predominant toxicants in sediments of Pohang and Yeongil Bay regions by use of EDA, and to enhance microalgal bioassays by applying cell viability assays using flow cytometry. Multiple species of microalgae, including the green algae, *Dunaliella tertiolecta*; haptophyte, *Isochrysis galbana*; and diatom, *Phaeodactylum tricornutum* with their various characteristics, such as morphotype, presence of cell walls, and motility, were tested individually to evaluate potential toxicants in whole and fractions of organic extracts of sediments (Borowitzka and Siva, 2007; Gallo et al., 2020). Specific objectives were to: (i) apply assays of cell viability using flow cytometry in EDA; (ii) evaluate the relationship between the inhibition of growth and cell viability; (iii) assess how target PAHs contribute to overall induced toxic responses; and finally (iv) identify potential algal toxicants in mixture sediments by use of GC-QTOFMS.

2. Materials and methods

2.1. Collection and preparations of samples

In previous studies, greater concentrations of organic and inorganic pollutants were reported to accumulate in sediments of the industrial areas of Pohang City compared to urban areas (Hong et al., 2014; Kim et al., 2014; Bailon et al., 2018). Thus, in the present study, we focused on contaminations by organic toxic substances and their potential microalgal toxicities in sediments from industrial hotspots. Surface sediments were collected during May 2018, from Gumu Creek (S1, industrial area), which flows into the Hyeongsan River, Hyeongsan River Estuary (S2), and Yeongil Bay (S3–S6) by use of a grab sampler (Fig. S1 of the Supplementary Materials). Samples were transported to the laboratory in pre-cleaned glass jars, then stored at −20 °C until analysis. Samples used for bioassays and chemical analyses were prepared by use of previously published methods (Hong et al., 2015). In brief, freeze-dried sediments were passed through a 1-mm sieve and homogenized. Forty grams of sediments were extracted using a Soxhlet extractor with 350 mL dichloromethane (DCM, J.T. Baker, Phillipsburg, NJ) for 16 h. Organic extracts were exchanged with hexane (Honeywell, Charlotte, NC), and elemental sulfur was removed using activated copper. Organic extracts were then concentrated to 4 mL with a rotary evaporator and N_2 gas (10 g sediment equivalents [SEq] mL^{-1}). Raw extracts (RE) were separated into two aliquots (1 mL and 3 mL) and used for bioassay and chemical analysis/further fractionations, respectively. The organic extract (1 mL) was exchanged with dimethyl sulfoxide (DMSO, Sigma-Aldrich, St. Louis, MO) for the bioassay. To avoid surrogate standards adversely affecting the bioassay, they were not added during sample preparations.

2.2. Silica gel and RP-HPLC fractionations

Eight grams of activated silica gel were packed into a glass column with hexane. RE was separated into three fractions based on polarity: non-polar (F1), aromatics (F2), and polar (F3). F1, F2, and F3 were eluted with 30 mL hexane, 60 mL of 20% DCM in hexane, and 50 mL of 40% acetone in DCM, respectively. One milliliter of silica gel fractions was separated into 10 sub-fractions according to log K_{OW} values using reverse-phase (RP)-HPLC (Agilent 1260 HPLC, Agilent Technologies, Santa Clara, CA) (Table S1) (Hong et al., 2016). Sub-fractions were exchanged with hexane or DMSO.

2.3. Inhibition of growth of microalgae

Three species of marine microalgae were used in this study. *D. tertiolecta* was obtained from NeoEnBiz Inc. (Bucheon, Korea). *I. galbana* and *P. tricornutum* were obtained from the Korea Marine Microalgae Culture Center (KMCC, KIOST, Geoje, Korea). *D. tertiolecta* and *P. tricornutum* are international standard species recommended for use by the American Society for Testing and Materials (ASTM) and International Organization for Standardization (ISO) (ISO10253, 2006; ASTM;E1218, 2012). Due to its relatively great sensitivity, *I. galbana* is also widely used in microalgal bioassays. Microalgae culture and bioassays were performed with some modifications to ISO 2006 (ISO10253, 2006). Detailed information on the culture conditions of the three microalgae is presented in Table S2. Microalgal bioassays were performed with algae cultured for 72–96 h and in the exponential growth phase. Test cultures were grown in 50-mL culture flasks with 8 mL culture medium. All experiments were performed in triplicates and included control and solvent control (0.1% DMSO). To minimize confounding effects of differences in intensities of lighting, flasks were randomly moved every 24 h. After 72 h exposure, numbers of cells were measured by direct cell counting under the light microscope (×400 Optical Microscope, Olympus, Tokyo, Japan) with a disposable hemocytometer (INCYTO, Cheonan, Korea). Intrinsic rate of growth (μ) and inhibition of growth ($I_{\mu i}$) were estimated (Eqs. 1 and 2):

$$\mu = \frac{\ln f_0(N_{72}) - \ln f_0(N_0)}{t_{72}} \quad (1)$$

$$I_{\mu i}(\%) = \frac{\overline{\mu}_C - \mu_i}{\overline{\mu}_C} \times 100 \quad (2)$$

Where N_0 is the initial cell density, and N_{72} is the cell density at the end of the test (72 h) in Eq. (1). For Eq. (2), μ_i is the growth rate for test flask i, and $\overline{\mu}_C$ is the mean growth rate for the control cultures (ISO10253, 2006).

2.4. Viability of microalgal cells

The cell viability assay was conducted using a BD FACS Canto II flow cytometer (BD Biosciences, San Jose, CA) equipped with three lasers (405 nm, 488 nm, and 633 nm) and eight filters. A 405 nm laser was used to analyze SYTOX blue (Thermo Fisher Scientific, Cambridge, UK). A 488 nm laser was used for fluorescein diacetate (FDA; Sigma-Aldrich) and propidium iodide (PI; Thermo Fisher Scientific). A 633 nm laser was used for Chl. *a*. Out of the eight filters, FS (forward scatter; cell size), SS (side scatter; intracellular complexity), Pacific Blue (SYTOX blue, 450/50 nm), FITC (FDA, 530/30 nm), PE (PI, 585/42 nm), and APC (Chl. *a*, 660/20 nm) were used to measure cell viability. For each sample, 5000 cells were measured; however, in cases where 5000 cells were not available, samples were measured for 5 min.

Before quantifications of numbers of cells, 6 mL of the experimental medium were centrifuged at 3500 rpm (1000 g) for 15 min *D. tertiolecta* and *I. galbana* were resuspended in 1 mL clean medium for double staining. Double staining with FDA and SYTOX blue was done, with some modifications, by use of previously published methods (Olsen et al., 2016). FDA is a measure of non-specific esterase activity and is used to distinguish live cells from dead cells. Hydrophilic FDA diffuses into living cells, and is cleaved by esterase to release fluorescein, which is fluorescent. Fluorescein is hydrophobic and cannot spread beyond the cell. Fluorescence of FDA is directly proportional to esterase activity. SYTOX blue stains occult nucleic acid (DNA and RNA), and diffuses into the membrane of damaged cells where it emits blue fluorescence. Thus, double staining with FDA and SYTOX blue allows viable cells and non-viable cells to be distinguished easily. First, the cells were stained for 15 min with FDA (in acetone) to a final concentration of 5 μM, and allowed to react in a darkroom. After FDA staining, cells were stained with SYTOX blue (in DMSO) to obtain a final concentration of 2 μM in a darkroom. For the positive control, cells were heat-treated in a 60 ℃ water bath for 1 h. Single staining of *P. tricornutum* was performed using FDA and PI. PI was used to indicate the same endpoint as SYTOX blue, has similar emission fluorescent are FDA when affected by chlorophyll *a* autofluorescence (Olsen et al., 2016). Thus, it was resuspended in 2 mL clean medium and separated into two aliquots for single staining. The cells in each aliquot were stained with FDA (in acetone) and PI (in distilled water) to obtain a final concentration of 30 μM and 5 μM in a darkroom, respectively.

Populations of cells were identified based on cell size and intracellular complexity, and were reconfirmed by measurement of Chl. *a*. Unstained, solvent control, and positive control cells are shown in Fig. S2. Double staining results were determined using quadrants (Q1, Q2, Q3, and Q4) by comparing the distribution of the solvent control and positive control in the dot plot of FDA and SYTOX blue (Fig. S2 and Table S3). Populations of the solvent control were determined by the control gate, which is not affected by exposure. The control gate was set to contain ≥ 90% cells (Fig. S2).

2.5. Targeted chemical analyses

Fifteen PAHs, 10 SOs, and 7 APs were analyzed as target pollutants. The full names of the target compounds are provided in Table S4. Targeted chemical analyses were performed with silica gel fractions. An internal standard (2-fluorobiphenyl, Chem Service) was added to each fraction before GC injection. An Agilent 7890B gas chromatograph equipped with a 5977B mass selective detector (MSD, Agilent Technologies) was used for quantification of PAHs, SOs, and APs. A 1 μL volume was injected onto a DB5MS column (30 m × 0.25 mm i.d. × 0.25 μm film). A detailed description on instrumental conditions is provided in Table S5. Recovery rates of surrogate standards raged from 89% to 110% (mean=100%) for Ace-d_{10}, from 86% to 99% (mean=93%) for Phe-d_{10}, from 82% to 89% (mean=87%) for Chr-d_{12}, and from 58% to 83% (mean=71%) for perylene-d_{12}. Method detection limits (MDL) for individual PAHs, SOs, and APs ranged from 0.39 to 2.1, from 0.01 to 3.9, and from 0.01 to 0.03 ng g^{-1} dm, respectively.

2.6. Full-scan screening analysis

FSA was performed using an Agilent 7890B gas chromatograph equipped with a 7200 QTOFMS (Agilent Technologies). One microliter of sample was injected onto a DB5MS column (30 m × 0.25 mm i.d. × 0.25 μm film). A detailed description of instrumental and analytical conditions are provided in Table S6. After GC-QTOFMS analysis for fractions with greater toxic potencies (F2.7 of S1) based on biotests, tentative algal toxicants were selected based on the match factor score (≥90%) of the spectral library (NIST library ver. 2014). Second, targeted PTSs in fractions were removed, including PAHs, SOs, and APs (Marsili, 2001; Booij et al., 2014). A matching score of ≥ 70% was considered acceptable for compounds in previous studies; however, the present study applied a more stringent standard because toxicity was not confirmed using standard materials (Sjollema et al., 2014; Gómez-Ramos et al., 2016; Cha et al., 2019; Kim et al., 2019). Instead, the compounds identified in fractions were evaluated for potential toxicity to algae, by use of an in silico method (ECOSAR v1.11) (US-EPA, 2012). The EC50, based on inhibition of growth, was predicted, and the least EC50 of the various compound groups in ECOSAR was used. Water solubility was predicted by WS Kowwin (v1.43), which is included in the ECOSAR package.

2.7. Confirmation of toxicity contribution by PAHs

To estimate the contribution of target PAHs to adverse effects on microalgal toxicity, a mixture of PAH standards (AM; artificial mixture) was prepared at the same concentrations of target compounds in F2.7

(more toxic fraction; details in Results and Discussion).

2.8. Data analysis and statistics

The data were analyzed using Flow Jo ver. 10 (Oregon, Ashland) single-cell analysis software. The percentage of cells outside the control gate was set to 0% in the solvent control. Significant differences with cells in the control gate and each quadrant were analyzed. The data were tested for normality using a Shapiro-Wilks test before subsequent analyses because of the limited sample size. Then, a *t*-test was carried out to determine the significant difference between the treatments. All statistical analyses (Shapiro–Wilks test, *t*-test, principal component analysis (PCA), and cluster analysis) were conducted using SPSS software (ver. 24.0, SPSS INC., Chicago, IL).

3. Results and discussion

3.1. Inhibition of growth of microalgae

Inhibitions of growth of three microalgae exposed to sediment REs and their fractions were measured. After 72 h exposure of *D. tertiolecta* and *I. galbana* to the sediment REs, inhibition of growths were not significantly different compared by solvent control (Fig. 1a). Growth of *P. tricornutum* was significantly different in REs of sites S1, S2, and S4, which was inhibited by 19%, 40%, and 21%, respectively. Silica gel fractionation was performed on the REs of S1, S2, and S4 (Fig. 1b). Growths of the three microalgae showed greater inhibition by exposure to the silica gel fractions of S1 than S2 and S4. The pattern of inhibition of growth after exposure to silica gel fractions of S1 differed among species of microalgae. For example, growth of *D. tertiolecta* was significantly inhibited by exposure to F2 (100%) and F3 (25%), but not to F1. Growth of neither *I. galbana* nor *P. tricornutum* was entirely inhibited (100%) by exposure to F2 or F3, while growth was less inhibited by F1. Thus, the three species of microalgae exhibited varied sensitivities to contaminants (Magnusson et al., 2008; Sjollema et al., 2014).

Greater inhibition of growth of microalgae by exposure to the silica gel fractions compared to corresponding REs might have been due to mixed toxic effects, leading to antagonistic reactions (Schwab et al., 2009). Greater toxicity to microalgae in fractions compared to REs has been reported previously (Grote et al., 2005; Schwab et al., 2009; Smital et al., 2011). Inhibition of growth of *Scenedesmus vacuolatus* by the aromatic fraction compared to that of the REs was about 30–40% greater (Grote et al., 2005; Schwab et al., 2009). Inhibition of growth of *Desmodesmus subspicatus* by polar and highly-polar fractions of the effluent of wastewater treatment plants were about 10−15% greater than raw wastewater (Smital et al., 2011). Results of a previous study suggested that resin compounds in sediment organic extract might adsorb hydrophobic organic compounds and reduce their toxic potencies to organisms (Schwab et al., 2009). Hence, a plausible explanation is that resin compounds could not be eluted in F3 of the silica gel column used in this study, and retained on the column.

Additional fractionations of F2 and F3 of S1 were conducted by use of RP-HPLC (Fig. 1c). Growth was inhibited more by F2 sub-fractions compared to F3 sub-fractions. Thus, toxicants that most affected algae were primarily contained in F2 (i.e., aromatic compounds). Of the F2 sub-fractions, growth of the three microalgae was generally inhibited by F2.6. Most potent fractions were species-specific; F2.6 (log K_{OW} 5–6) for *D. tertiolecta,* F2.6–F2.8 (log K_{OW} 5–8) for *I. galbana*, and F2.5–F2.7 (log K_{OW} 4–7) for *P. tricornutum*. The main toxicants inhibiting growth differed among species of microalgae, which is caused by characteristics of each microalgal species, such as cell size, surface area, uptake into cells, and the presence or absence of cell walls (Weiner et al., 2004; Borowitzka and Siva, 2007; Othman et al., 2012; Lee et al., 2020). Exposure of *D. tertiolecta* and *I. galbana* to certain F3 sub-fractions (F3.5 and F3.6) resulted in slight inhibition of growth, with no specific fraction showing strong toxicity being isolated. Thus, chemicals toxic to microalgae likely exist over a wide range of fractions or show mixed toxic effects (i.e., synergistic effects).

3.2. Inhibition of viability of cells

First, results of previous studies related to the toxicity evaluation

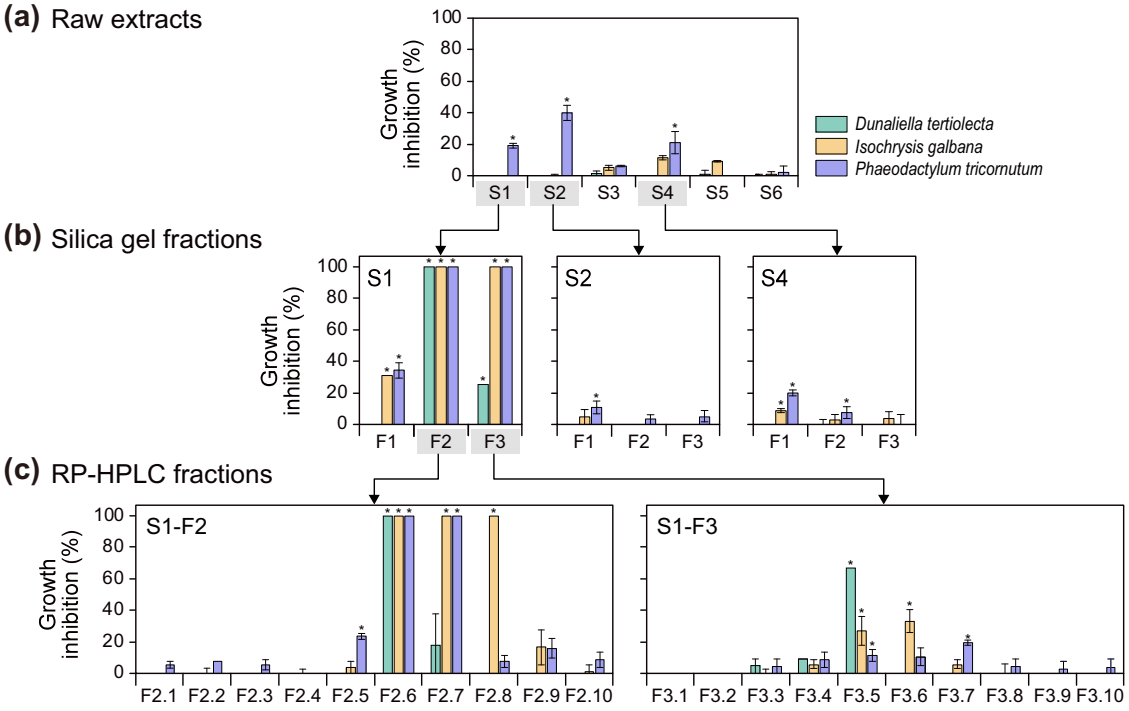

Fig. 1. Inhibition of growth of three microalgae after exposures to: (a) raw organic extracts, (b) silica gel fractions, and (c) RP-HPLC fine fractions of sediments from Yeongil Bay, Korea (*: significantly different compared by solvent control; $p < 0.05$).

using microalgal bioassays were reviewed (Table S7). Assays of viability of cells have been mostly applied in studies about the physiological responses by exposure of pure chemicals. In studies evaluating potential toxicity of environmental samples using microalgae, inhibition of growth was generally used as the measurement endpoint. Among EDAs using microalgal bioassays, there are very few studies on which assays of viability of cells have been applied. In the present study, we focused on evaluating the potential toxicity by organic pollutants in sediments using the cell viability assays, which would provide more detailed information on the causative toxic substances in environments.

Esterase activity of *D. tertiolecta* was only minimally inhibited by exposure to the RE of S1, while inhibition of viability of cells exposed to

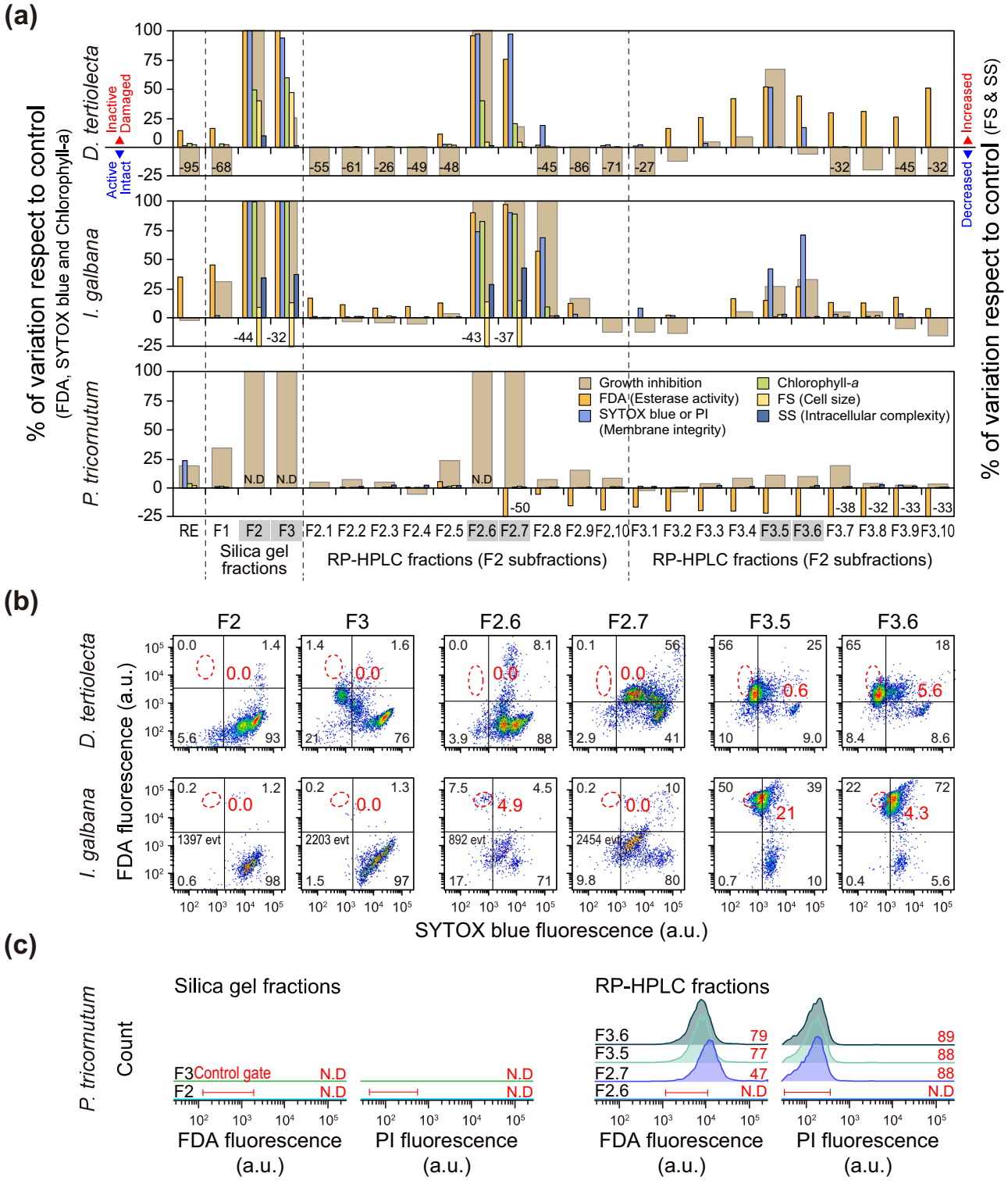

Fig. 2. Results of microalgal assays after exposures to the raw organic extracts and fractions (silica gel and RP-HPLC) of sediment from site S1. (a) Inhibition of growth and cell viability (percent of inhibitions compared to solvent control; FDA values increase with inhibition of esterase activity and SYTOX blue (or PI) values increase with damage of cell membrane), (b) flow cytometry dot plots of *D. tertiolecta* and *I. galbana* cells with FDA and SYTOX blue, and (c) fluorescence histograms of *P. tricornutum* cells with FDA and PI.

silica gel fractions was observed (Fig. 2a). For example, viability of *D. tertiolecta* was significantly inhibited and accompanied by lesser esterase activity, membrane damage, lesser Chl. *a*, and greater cell size when exposed to F2 and F3 of S1. Of the F2 sub-fractions, viability of *D. tertiolecta* was inhibited by exposure to F2.6 and F2.7. Growth of *D. tertiolecta* was slightly inhibited (18%) by exposure to F2.7 of S1, but esterase activity and cell membrane damage were strongly inhibited by the sample (About 41% of cells distributed in Q4 in dot plot) (Fig. 2b). Of the F3 sub-fractions, F3.3−F3.10 inhibited esterase activity, while exposure to F3.5 and F3.6 damaged membranes. For the RE and F3.3−F3.10, excluding F3.5, rates of growth were inversely proportional to esterase activity (Table S8). This response indicated hormesis, which is an abnormal increase in growth that occurs when toxic substances are present at concentrations less than those inducing inhibition of growth (Calabrese, 1999).

Esterase activity of *I. galbana* was inhibited by exposure to RE of S1 (Figs. 2a and S3). *I. galbana* after exposures to silica gel fractions, F2 and F3 exhibited significantly lesser viability of cells compared to solvent control (Fig. 2a and b). Toxic responses of *I. galbana* were observed when exposed to F2.6−F2.8 and F3.5−F3.6. In particular, F2.6 and F2.7 inhibited all endpoints associated with viability of cells. However, F2.8 only inhibited esterase activity and damaged cell membranes. The population of *I. galbana* in Q4 when exposed to F2.6, F2.7, and F2.8 was 71%, 80%, and 25%, respectively (Fig. 2a and S3 and Table S9).

Viability of *P. tricornutum* could not be evaluated because all cells were dead after exposure to F2, F3, and F2.6 of S1 (Fig. 2a and c), the fractions which caused 100% inhibition of growth. However, it was possible to evaluate cell viability exposed to F2.7, with an increase of esterase activity in *P. tricornutum*. When *P. tricornutum* was exposed to sub-fractions F3.5−F3.10, esterase activity increased more than 20% compared to solvent control (Table S10). Results of previous studies have shown that esterase activity might increase as a result of accumulation of enzymes stopping cell separation and/or cell defense mechanisms at early stage of toxic responses, or under weak toxic pressure (Xue et al., 2018; Machado and Soares, 2019). However, it was difficult to discern specific toxic mechanisms of microalgae from the results of this study; further study on this phenomenon is needed in the future.

Results of assays of inhibition of growth and viability of cells collectively indicated that three microalgal species possess chemical-specific responsiveness. For example, among the 10 sub-fractions of F2 of S1, microalgal toxicities were specifically linked to certain fractions; F2.6 and F2.7 for *D. tertiolecta* and *P. tricornutum*, and F2.6−F2.8 for *I. galbana*. F2.6 and F2.7 include aromatics with log K_{OW} 5−7, particularly PAHs, which are well known to be toxic to algae (Bandow et al., 2009; Schwab et al., 2009). PAHs are adsorbed onto and damage cell membranes of microalgae, which prevents uptake of nutrients, consequently lead inhibition of photosynthesis (Fan and Reinfelder, 2003; Aksmann and Tukaj, 2008; Othman et al., 2012; Cerezo et al., 2017). Sensitivities or efficacy of responses among species of microalgae could be related to sizes of their cells, which influences surface areas of cells. For example, due to the relatively large cell size, viability and growth of *D. tertiolecta* would be less sensitive to hydrophobic compounds compared to other species (Table S2). It has been documented to be less sensitive to PAHs than other marine microalgae species and less sensitive to polychlorinated biphenyls (PCBs) than diatoms (Mosser et al., 1972; Okumura et al., 2003).

Since esterase activities were inhibited over a wide range of F3 sub-fractions, specific toxic fractions were not isolated (Fig. 2a). Following exposure to F3 sub-fractions, greater esterase activity of *P. tricornutum* was not accompanied by significant inhibition of growth, but was considered to be an early stage of toxicity (Xue et al., 2018). Thus, *D. tertiolecta* was more sensitive to the effects of F3 sub-fractions compared to *P. tricornutum*. Toxicity is closely related to uptake of toxic substances, which are species-specific (Weiner et al., 2004). In addition, *P. tricornutum* is a diatom with a hard silicate cell wall. The hard cell walls of *P. tricornutum* influence the uptake of and interaction of toxic substances (Gallo et al., 2020; Lee et al., 2020). Overall, polar toxicants tend to be absorbed better by *D. tertiolecta* compared to *I. galbana* or *P. tricornutum*.

3.3. Relationship between inhibition of growth and cell viability

Relationships between endpoints of toxicity to microalgae were evaluated statistically, along with comparisons between species. PCA showed that growth and cell viability of *D. tertiolecta* and *I. galbana* were inhibited after exposure to REs and fractions, with four groups being delineated (A−D) (Fig. 3a). Group A included solvent control and less toxic fractions, which did not inhibit growth, but did inhibit esterase activity, for the three species. Inhibition of esterase activity was documented to be a sensitive endpoint that is commonly observed at the early stages of toxic responses in microalgal bioassay (Gosset et al., 2019), which was also evidenced in the present study. Damage of cell membranes was observed for groups B and C, which also caused inhibition of growth, but less sensitive than inhibition of esterase activity. Group D included fractions F2, F3, and some F2 sub-fractions, which were more potent to *D. tertiolecta* and *I. galbana*. For example, Group D samples apparently caused the maximum inhibition of growth (100%) and also affected all the endpoints related to cell viability, such as Chl. *a*, cell size, and intracellular complexity. Thus, these parameters can be suitable endpoints capable of distinguishing greater toxic effects even when inhibition of growth prevailed (Prado et al., 2011).

Results of cluster analysis revealed three representative groups reflecting the characteristics of inhibition of growth and cell viability, with indication of species-specific sensitivity (Fig. 3b). Chl. *a*, cell size, and intracellular complexity were clustered in *D. tertiolecta* and *I. galbana*. However, other endpoints were grouped differently for these two species. For instance, inhibition of esterase activity and damage to membranes were grouped in *D. tertiolecta*, while inhibition of growth was distinguished, and inhibition of growth and damage to membranes were grouped in *I. galbana*. Such endpoint-specific grouping might be attributed to differences in damage to membranes of the two species. Damage to membranes of microalgae is generally recognized as an initial effect of apoptosis; however, *D. tertiolecta* has been reported to sustain growth of cells, even when membranes are damaged (Ellis et al., 1991; Segovia and Berges, 2009). Esterase activity tended to be inhibited during early stages of responses for *D. tertiolecta* and *I. galbana*. However, growth was maintained in *D. tertiolecta* even after damage to membranes occurred; *D. tertiolecta* exhibited little inhibition of growth compared to that in *I. galbana*. Thus, the different response of growth by damage of membranes was reflected that *I. galbana* showed significant inhibition of growth to more fractions of sediment RE compared to *D. tertiolecta*.

Cell viability data for fractions F2, F3, and F2.6 were not available for *P. tricornutum*, and thus were excluded from the statistical analysis. In the PCA, fractions formed three groups (A−C) based on inhibition of growth and esterase activity. Damage to membranes, Chl. *a*, cell size, and intracellular complexity were grouped, but explained little of toxic potencies of fractions of sediment extracts. Cluster analysis showed a similar trend to PCA. Cell membrane damage, Chl. *a*, cell size, and intracellular complexity were grouped, while the inhibition of growth and esterase activity fell into separate groups. Because *P. tricornutum* has a hard cell wall, it does not change cell size and density substantially when stressed by toxic substances compared to other species (Borowitzka and Siva, 2007; Zhuravel et al., 2009). Thus, effects on esterase activity and growth inhibition may be more pronounced than other endpoints in cell viability assay for *P. tricornutum*.

3.4. Contamination of PTSs in sediments

The greatest concentrations of PAHs were observed in S1, followed by S2, S5, S4, S3, and S6 (Table S4 for details). Concentrations of ΣPAHs

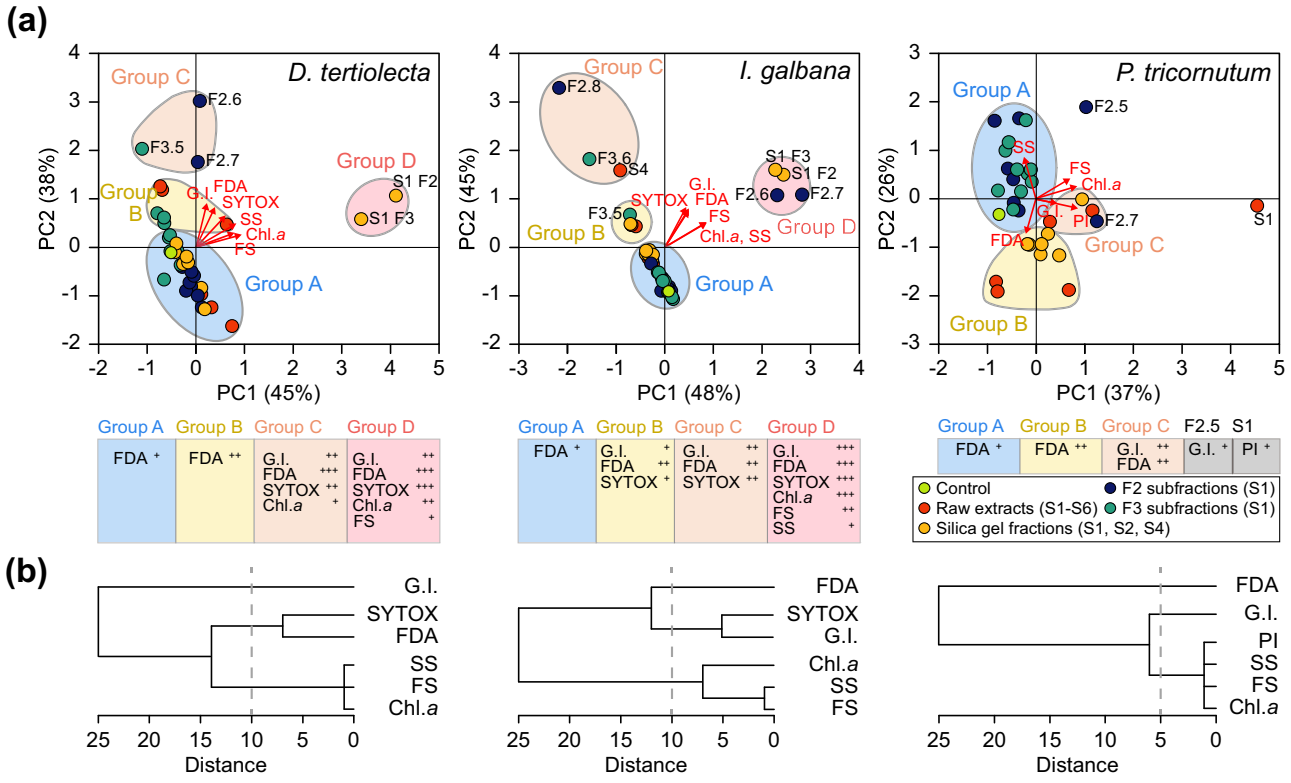

Fig. 3. (a) PCA biplots of the three microalgal species and (b) cluster analysis results based on inhibition of growth and cell viability inhibition. Groups were delineated based on the observed toxic responses of each endpoint. The box below the PCA plots indicates the endpoints affected by the groups or fractions (+: 20−50% cells were distributed outside the control gate; ++: 50−80% cells were distributed outside the control gate; and +++: 80−100% cells were distributed outside the control gate).

in extracts of S1 were 220,000 ng g^{-1} dry mass (dm) and were dominated by 4 – 6 ring PAHs. Concentrations of individual PAHs in S1 exceeded probable effect levels (PELs) delineated by the CCME (CCME, 2001). In particular, compared to PEL, concentrations of phenanthrene (Phe) and pyrene (Py), which are well-known microalgal toxicants, were 103- and 17-times greater, respectively (Table S11) (CCME, 2001; Echeveste et al., 2010).

The EC50 of acenaphthene (Ace), fluorene (Flu), Phe, antracene (Ant), fluoranthene (Fl), Py, benzo[*a*]anthracene (BaA), and benzo[*a*] pyrene (BaP) to inhibit growth of at least one species of microalgal used in the present study was documented to range from 65 to 1800 μg L^{-1} (Table S12). Considering the exposure concentration of the organic extract of S1 on three microalgae, Fl for *D. tertiolecta*, Flu, Phe, Ant, Fl, and BaP for *I. galbana*, and Fl and Py for *P. tricornutum* exceeded the reported EC50 for inhibition of growth (Table S12). Out of these compounds, Fl, Py, and BaA were mainly eluted in F2.6, while BaP was mainly eluted in F2.7. Thus, Fl and Py may be main contributors to the toxic potency of F2.6 of S1 to microalgae. However, of the compounds eluted in F2.7, EC50 of BaP was only reported based on inhibition of growth of *I. galbana*.

To assess potential sources of PAHs, diagnostic ratios were used, such as Ant/(Ant+Phe), Flu/(Flu+Py), BaA/(BaA+ Chrysene), and Indeno [*1,2,3-cd*]pyrene (IcdP)/(IcdP+ Benzo[*g,h,i*]perylene) (data not shown). Diagnostic ratios indicated that most PAHs in Pohang area were of pyrogenic origin, including from combustions of coal, wood, and grass. Compared to results of previous studies conducted in the same area, contamination with PAHs is still serious (2400 ng g^{-1} dm in 2001 and 2100−4200 ng g^{-1} dm in 2010) (Koh et al., 2004; Hong et al., 2014). Source of PAHs identified in the present study generally supported the assessment of sediment contamination by PAHs in the previous studies.

Concentrations of SOs in sediments around Pohang ranged from 38 to 150 ng g^{-1} dm. The greatest concentration of SOs was detected in S1. SOs are emerging pollutants (Hong et al., 2016) with no comparative data available in the study area. Compared to other industrial areas of Korea, such as Lake Sihwa (89−870 ng g^{-1} dm) and Ulsan Bay (36−3700 ng g^{-1} dm) (Cha et al., 2019; Kim et al., 2019), SOs in sediments did not appear to be severely contaminated in Pohang and Yeongil Bay regions. Thus, SOs are unlikely to have significant adverse effects on microalgae; however, these PTSs occurred in toxic fractions (e.g., F2.6 and F2.7); thus, further research on the potential toxicity of SOs are needed. Concentrations of APs in sediments ranged from 2.0 to 98 ng g^{-1} dm, which did not exceed existing sediment quality guidelines, such as ISQG (1000 ng g^{-1}) (2001). The concentration of APs, like other PTSs, was the greatest in S1, with this tributary appearing to be a hotspot of PTSs in the study area. APs were eluted in F3, but did not seem to contribute significantly to toxicity to microalgae in F3. This is because concentrations that cause toxic effects, such as inhibition of growth to *I. galbana*, were of a certain level (μg L^{-1}) (Tato et al., 2018), with concentrations of APs in sediments being lesser. Relative toxicities of target compounds on microalgae were compared using toxic potencies derived from the linear free energy model, ECOSAR (Table S13). Results indicated that SOs and APs had similar or slightly lesser EC50 values compared to those of PAHs. However, concentrations of PAHs in sediments were significantly greater than those of SOs and APs; thus, the toxicity contributions of SOs and APs were considered to be less than those by PAHs (Table S4).

3.5. Contributions of targeted PAHs to toxic potency

To determine relative contributions of individual PAHs to toxic potencies in F2.7 of S1 toward microalgae, a test medium containing a mixture of standard materials for six PAHs (benzo[*b*]fluoranthene, benzo[*k*]fluoranthene, BaP, IcdP, dibenz[*a,h*]anthracene, and BghiP) was prepared (Fig. 4 and Table S14). Concentrations of these PAHs were

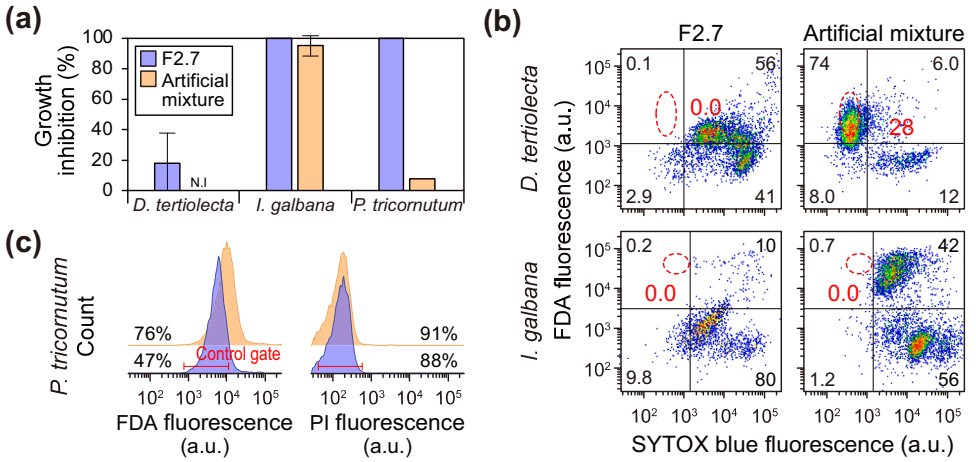

Fig. 4. (a) Inhibition of growth of the three microalgae after exposure to the F2.7 fraction and artificial PAH mixture (N.I: non-inhibition), (b) flow cytometry dot plots of *D. tertiolecta* and *I. galbana* cells with FDA and SYTOX blue, and (c) fluorescence histograms of *P. tricornutum* cells with FDA and PI.

greater than their limits of aqueous solubility, because DMSO was applied as a carrier solvent (0.1% dose). When exposed to hydrophobic compounds at concentrations greater than their aqueous solubility: 1) distributions of compounds in the test medium becomes inhomogeneous, and 2) the compounds are lost by adsorption to plastic materials and organisms, volatilization, or metabolism with potential toxicity being underestimated (Smith et al., 2010; Kwon and Kwon, 2012; Niehus et al., 2018). This problem also occurs in exposures of microalgae from sediment organic extracts. However, because the present study evaluated contributions of target PAHs to toxic potencies to microalgae caused by exposure in the F2.7 of S1, the exposure concentration of AM was given by assuming that PAHs in the F2.7 of S1 were completely diluted in the exposure medium.

Exposure of the three microalgae to AM showed that inhibition of growth of *D. tertiolecta* and *I. galbana* was non-significantly different to the F2.7 of S1 (Fig. 4a). However, inhibition of growth of *P. tricornutum* after exposure to AM was relatively small compared to that of the F2.7 of S1. Thus, these compounds did not fully explain inhibition of growth of *P. tricornutum* by F2.7 of S1. Based on flow cytometry, the population of *D. tertiolecta* in Q1 (healthy cells) was significantly larger following exposure to AM (74%) compared to that of F2.7 of S1 (0.1%) (Fig. 4b). Thus, inhibition of cell viability of *D. tertiolecta* in F2.7 was only partially explained by detected concentrations of PAHs. Damage to membranes of *I. galbana* in F2.7 was explained well by targeted PAHs, while inhibition of esterase activity was partly explained. Inhibition of Chl. *a*, cell size, and intracellular complexity might occur following inhibition of growth of *I. galbana* and was detected after AM exposure (Table S15). However, inhibition of Chl. *a*, cell size, and intracellular complexity by exposure to AM was not as great as responses to F2.7 of S1. Targeted PAHs accounted for part of the observed inhibition of esterase activity caused by F2.7 of S1 for *P. tricornutum*, while as for F2.7, no damage to membranes was observed (Fig. 4c).

3.6. Full-scan screening analysis

FSA was conducted to identify unknown microalgal toxicants in the F2.7 of S1 by use of GC-QTOFMS. In total, 294 compounds were detected in the F2.7 of S1, and were matched to the NIST Library (ver. 2014). After removing targeted PAHs, 58 compounds were selected as tentative toxicants based on the matching score (≥90) (Table 1 and S16). Toxic potencies of these compounds were evaluated by use of ECOSAR based on EC50 for inhibition of growth of the freshwater green algae, *Raphidocelis subcapitata*. The compounds of lesser EC50 values than target compounds were PAHs that primarily originated from combustion of coal and wood as well as byproducts of liquefaction of coal (Oros and Simoneit, 2000; Zhao et al., 2008; Zheng et al., 2020). 1-Phenylpyrene, dibenz[*a*,*c*]anthracene, and picene were predicted to be the top three ranked toxic substances in the sediment sample. The EC50 of these compounds for inhibition of growth was comparable to those of IcdP, DbahA, and BghiP (EC50: 0.054 mg L^{-1} predicted in ECOSAR). These substances seemed to originate from surrounding industrial complexes, including steel and steel-related industries. In the future, it is necessary

Table 1
Potential microalgal toxicants in the most potent fraction (F2.7 of S1) (Compounds of lesser EC50 values than target compounds based on the predicted EC50 for inhibition of growth using ECOSAR).

CAS#	Compound name	Formula	EC50 (mg L^{-1})	Uses/origins	References
5101–27–9	1-Phenylpyrene	$C_{22}H_{14}$	0.054[a]	Byproducts of coal liquefaction	Zheng et al. (2020)
215–58–7	Dibenz[*a*,*c*]anthracene	$C_{22}H_{14}$	0.054[a]	–	
213–46–7	Picene	$C_{22}H_{14}$	0.054[a]	Coal combustion	Oros and Simoneit (2000)
193–39–5	Indeno[*1,2,3-cd*]pyrene[b]	$C_{22}H_{12}$	0.054[a]		
53–70–3	Dibenz[*a*,*h*]anthracene[b]	$C_{22}H_{14}$	0.054[a]		
191–24–2	Benzo[*g*,*h*,*i*]perylene[b]	$C_{22}H_{12}$	0.054[a]		
63,104–32–5	10-Methylbenzo[*a*]pyrene	$C_{21}H_{14}$	0.055[a]	Byproducts of coal liquefaction	Zheng et al. (2020)
57,652–66–1	4,5-Dihydrobenzo[*a*]pyrene	$C_{20}H_{14}$	0.067[a]	–	
239–85–0	13 H-Dibenzo[*a*,*h*]fluorene	$C_{21}H_{14}$	0.088[a]	Components of coal	Zhao et al. (2008)
50,861–05–7	9 H-Cyclopenta[*a*]pyrene	$C_{19}H_{12}$	0.105[a]	–	
198–55–0	Perylene	$C_{20}H_{12}$	0.125[a]	Components of coal	Zhao et al. (2008)
225–99–2	Benzo[*b*]fluoranthene[b]	$C_{20}H_{12}$	0.125[a]		
207–08–9	Benzo[*k*]fluoranthene[b]	$C_{20}H_{12}$	0.125[a]		
50–32–8	Benzo[*a*]pyrene[b]	$C_{20}H_{12}$	0.125[a]		

[a] Exceeds predicted water solubility by WS Kowwin (v1.43) included in the ECOSAR program.
[b] Target compounds in F2.7 fraction.

to develop the novel water and air treatment technology to prevent the introduction of causative toxic substances originating from the industrial complexes into the aquatic environments (Maleki et al., 2016; Maleki, 2018; Kara et al., 2020; Rahimi et al., 2020). Of note, ECOSAR is based on a linear mathematical relationship between log K_{OW} and measured toxicity values in each chemical class training set, it has limited to predicting for the substance that are difficult to determine the chemical class or have unique mode of toxic actions (Moore et al., 2003; Mayo-Bean et al., 2012). Further studies on the ecotoxicological effects and confirmation of predicted toxicities for these compounds are necessary. In addition, a new index to assess the potential toxicities of contaminants in sediments based on diverse microalgal species with multiple endpoints can be developed; it will aid a more accurate risk assessment of hazardous substances in the aquatic and/or marine environments.

4. Conclusions

This study performed standard assays of inhibition of growth combined with a cell viability assay of microalgae encompassing three different taxa. Cell viability analysis enhanced our understanding of the physiological responses of single cells, and provided detailed toxic information that could not be obtained using the standard assay for inhibition of growth. In addition, FSA was very useful in identifying potential unknown toxic substances present in the toxic fractions. Further studies on the distribution, source, fate, and ecotoxicity of the suggested tentative toxic compounds would be required. In addition, environmental relevance could be improved by applying sampling and dosing techniques that should consider bioavailability. Despite some limitations, the microalgal bioassay combined with cell viability analysis applied in sediment EDA work represents a useful approach towards advancement of current EDA practices.

CRediT authorship contribution statement

Seong-Ah An: Conceptualization, Investigation, Formal analysis, Data curation, Visualization, Writing - original draft. **Seongjin Hong:** Conceptualization, Writing - original draft, Writing - review & editing, Project administration, Funding acquisition, Supervision. **Junghyun Lee:** Investigation, Formal analysis, Data curation, Writing - review & editing. **Jihyun Cha:** Investigation, Formal analysis, Data curation. **Sunggyu Lee:** Investigation, Formal analysis, Data curation. **Hyo-Bang Moon:** Conceptualization, Writing - review & editing. **John P. Giesy:** Conceptualization, Writing - review & editing. **Jong Seong Khim:** Conceptualization, Writing - review & editing, Funding acquisition, Supervision.

Declaration of Competing Interest

The authors declare that they have no known competing financial interests or personal relationships that could have appeared to influence the work reported in this paper.

Acknowledgments

This work was supported by the project entitled “Development of techniques for assessment and management of hazardous chemicals in the marine environment (2014–0342)” funded by the Ministry of Oceans and Fisheries of Korea. This work was also supported by the National Research Foundation of Korea (NRF) grant funded by the Korean government (MSIP) (2016R1E1A1A01943004, 2017R1E1A1A01075067, and 2020R1A4A2002823). Prof. Giesy was supported by the Canada Research Chair program of the Natural Sciences and Engineering Research Council of Canada and a distinguished visiting professor in Environmental Sciences at Baylor University.

Appendix A. Supporting information

Supplementary data associated with this article can be found in the online version at doi:10.1016/j.jhazmat.2020.124230.

References

Aksmann, A., Tukaj, Z., 2008. Intact anthracene inhibits photosynthesis in algal cells: a fluorescence induction study on *Chlamydomonas reinhardtii* cw92 strain. Chemosphere 74, 26–32. https://doi.org/10.1016/j.chemosphere.2008.09.064.

Almeida, A.C., Gomes, T., Habuda-Stanić, M., Lomba, J.A.B., Romić, Ž., Turkalj, J.V., Lillicrap, A., 2019. Characterization of multiple biomarker responses using flow cytometry to improve environmental hazard assessment with the green microalgae *Raphidocelis subcapitata*. Sci. Total Environ. 687, 827–838. https://doi.org/10.1016/j.scitotenv.2019.06.124.

ASTM;E1218, 2012. Standard Guide for Conducting Static Toxicity Tests with Microalgae, 2012. ASTM International, West Conshohocken, PA. ⟨https://compass.astm.org/EDIT/html_annot.cgi?E1218+04(2012)#s00095⟩.

Bailon, M.X., David, A.S., Park, Y., Kim, E., Hong, Y., 2018. Total mercury, methyl mercury, and heavy metal concentrations in Hyeongsan River and its tributaries in Pohang City, South Korea. Environ. Monit. Assess. 190, 274. https://doi.org/10.1007/s10661-018-6624-4.

Baldetorp, B., Dalberg, M., Holst, U., Lindgren, G., 1989. Statistical evaluation of cell kinetic data from DNA flow cytometry (FCM) by the EM algorithm. Cytometry 10, 695–705. https://doi.org/10.1002/cyto.990100605.

Bandow, N., Altenburger, R., Streck, G., Brack, W., 2009. Effect-directed analysis of contaminated sediments with partition-based dosing using green algae cell multiplication Inhibition. Environ. Sci. Technol. 43, 7343–7349. https://doi.org/10.1021/es901351z.

Béchet, Q., Laviale, M., Arsapin, N., Bonnefond, H., Bernard, O., 2017. Modeling the impact of high temperatures on microalgal viability and photosynthetic activity. Biotechnol. Biofuels 10, 136. https://doi.org/10.1186/s13068-017-0823-z.

Bergmann, A.J., Tanguay, R.L., Anderson, K.A., 2017. Using passive sampling and zebrafish to identify developmental toxicants in complex mixtures. Environ. Toxicol. Chem. 36, 2290–2298. https://doi.org/10.1002/etc.3802.

Booij, P., Vethaak, A.D., Leonards, P.E.G., Sjollema, S.B., Kool, J., de Voogt, P., Lamoree, M.H., 2014. Identification of photosynthesis inhibitors of pelagic marine algae using 96-well plate microfractionation for enhanced throughput in effect-directed analysis. Environ. Sci. Technol. 48, 8003–8011. https://doi.org/10.1021/es405428t.

Borowitzka, M.A., Siva, C.J., 2007. The taxonomy of the genus *Dunaliella* (Chlorophyta, Dunaliellales) with emphasis on the marine and halophilic species. J. Appl. Psychol. 19, 567–590. https://doi.org/10.1007/s10811-007-9171-x.

Brack, W., 2003. Effect-directed analysis: a promising tool for the identification of organic toxicants in complex mixtures? Anal. Bioanal. Chem. 377, 397–407. https://doi.org/10.1007/s00216-003-2139-z.

Brack, W., Bandow, N., Schwab, K., Schulze, T., Streck, G., 2009. Bioavailability in effect-directed analysis of organic toxicants in sediments. TrAC Trends Anal. Chem. 28, 543–549. https://doi.org/10.1016/j.trac.2009.02.010.

Brack, W., Ait-Aissa, S., Burgess, R.M., Busch, W., Creusot, N., Di Paolo, C., Escher, B.I., Mark Hewitt, L., Hilscherova, K., Hollender, J., Hollert, H., Jonker, W., Kool, J., Lamoree, M., Muschket, M., Neumann, S., Rostkowski, P., Ruttkies, C., Schollee, J., Schymanski, E.L., Schulze, T., Seiler, T.-B., Tindall, A.J., De Aragão Umbuzeiro, G., Vrana, B., Krauss, M., 2016. Effect-directed analysis supporting monitoring of aquatic environments — an in-depth overview. Sci. Total Environ. 544, 1073–1118. https://doi.org/10.1016/j.scitotenv.2015.11.102.

Burkiewicz, K., Synak, R., Tukaj, Z., 2005. Toxicity of three insecticides in a standard algal growth inhibition test with *Scenedesmus subspicatus*. B. Environ. Contam. Toxicol. 74, 1192–1198. https://doi.org/10.1007/s00128-005-0707-y.

Calabrese, E.J., 1999. Evidence that hormesis represents an “Overcompensation” response to a disruption in homeostasis. Ecotoxicol. Environ. Saf. 42, 135–137. https://doi.org/10.1006/eesa.1998.1729.

Dupraz, V., Ménard, D., Akcha, F., Budzinski, H., Stachowski-Haberkorn, S., 2019. Toxicity of binary mixtures of pesticides to the marine microalgae *Tisochrysis lutea* and *Skeletonema marinoi*: substance interactions and physiological impacts. Aquat. Toxicol. 211, 148–162. https://doi.org/10.1016/j.aquatox.2019.03.015.

Echeveste, P., Agustí, S., Dachs, J., 2010. Cell size dependent toxicity thresholds of polycyclic aromatic hydrocarbons to natural and cultured phytoplankton populations. Environ. Pollut. 158, 299–307. https://doi.org/10.1016/j.envpol.2009.07.006.

Ellis, R.E., Yuan, J., Horvitz, H.R., 1991. Mechanisms and functions of cell death. Annu. Rev. Cell. Biol. 7, 663–698. https://doi.org/10.1146/annurev.cb.07.110191.003311.

Emelogu, E.S., Seiler, T.-B., Pollard, P., Robinson, C.D., Webster, L., McKenzie, C., Heger, S., Hollert, H., Bresnan, E., Best, J., Moffat, C.F., 2014. Evaluations of combined zebrafish (*Danio rerio*) embryo and marine phytoplankton (*Diacronema lutheri*) toxicity of dissolved organic contaminants in the Ythan catchment, Scotland, UK. Environ. Sci. Pollut. Res. 21, 5537–5546. https://doi.org/10.1007/s11356-013-2488-x.

Eudey, T.L., 1996. Statistical considerations in DNA flow cytometry. Stat. Sci. 11, 320–334. ⟨https://www.jstor.org/stable/2246028⟩.

Fan, C.-W., Reinfelder, J.R., 2003. Phenanthrene accumulation kinetics in marine diatoms. Environ. Sci. Technol. 37, 3405–3412. https://doi.org/10.1021/es026367g.

Franqueira, D., Orosa, M., Torres, E., Herrero, C., Cid, A., 2000. Potential use of flow cytometry in toxicity studies with microalgae. Sci. Total. Environ. 247, 119–126. https://doi.org/10.1016/S0048-9697(99)00483-0.

Funahashi, M., Hanna, J.-i, 1997. Fast ambipolar carrier transport in smectic phases of phenylnaphthalene liquid crystal. Appl. Phys. Lett. 71, 602–604. https://doi.org/10.1063/1.119806.

Gómez, M.J., Gómez-Ramos, M.M., Agüera, A., Mezcua, M., Herrera, S., Fernández-Alba, A.R., 2009. A new gas chromatography/mass spectrometry method for the simultaneous analysis of target and non-target organic contaminants in waters. J. Chromatogr. A 1216, 4071–4082. https://doi.org/10.1016/j.chroma.2009.02.085.

Gosset, A., Durrieu, C., Barbe, P., Bazin, C., Bayard, R., 2019. Microalgal whole-cell biomarkers as sensitive tools for fast toxicity and pollution monitoring of urban wet weather discharges. Chemosphere 217, 522–533. https://doi.org/10.1016/j.chemosphere.2018.11.033.

Grote, M., Brack, W., Altenburger, R., 2005. Identification of toxicants from marine sediment using effect-directed analysis. Environ. Toxicol. 20, 475–486. https://doi.org/10.1002/tox.20135.

Guo, J., Deng, D., Wang, Y., Yu, H., Shi, W., 2019. Extended suspect screening strategy to identify characteristic toxicants in the discharge of a chemical industrial park based on toxicity to *Daphnia magna*. Sci. Total Environ. 650, 10–17. https://doi.org/10.1016/j.scitotenv.2018.08.215.

Hernández, F., Sancho, J.V., Ibáñez, M., Abad, E., Portolés, T., Mattioli, L., 2012. Current use of high-resolution mass spectrometry in the environmental sciences. Anal. Bioanal. Chem. 403, 1251–1264. https://doi.org/10.1007/s00216-012-5844-7.

Hollender, J., Rothardt, J., Radny, D., Loos, M., Epting, J., Huggenberger, P., Borer, P., Singer, H., 2018. Comprehensive micropollutant screening using LC-HRMS/MS at three riverbank filtration sites to assess natural attenuation and potential implications for human health. Water Res. X 1, 100007 https://doi.org/10.1016/j.wroa.2018.100007.

Hong, S., Khim, J.S., Park, J., Kim, S., Lee, S., Choi, K., Kim, C.-S., Choi, S.-D., Park, J., Ryu, J., Jones, P.D., Giesy, J.P., 2014. Instrumental and bioanalytical measures of dioxin-like compounds and activities in sediments of the Pohang Area, Korea. Sci. Total Environ. 470–471, 1517–1525. https://doi.org/10.1016/j.scitotenv.2013.06.112.

Hong, S., Lee, J., Lee, C., Yoon, S.J., Jeon, S., Kwon, B.-O., Lee, J.-H., Giesy, J.P., Khim, J. S., 2016. Are styrene oligomers in coastal sediments of an industrial area aryl hydrocarbon-receptor agonists? Environ. Pollut. 213, 913–921. https://doi.org/10.1016/j.envpol.2016.03.025.

ISO10253, 2006. Water Quality-Marine Algal Growth Inhibition Test With *Skeletonema Costatum* and *Phaeodactylum Tricornutum*. International Organization for Standardization, Switzerland.

CCME, 2001. Canadian sediment quality guidelines for the protection of aquatic life summary table, in: Canadian environmental quailty guidelines, 1999, Canadian Council of Ministers of the Environment, Winnipeg. ⟨https://www.elaw.org/system/files/sediment_summary_table.pdf⟩.

Cerezo, M.I., Linden, M., Agustí, S., 2017. Flow cytometry detection of planktonic cells with polycyclic aromatic hydrocarbons sorbed to cell surfaces. Mar. Pollut. Bull. 118, 64–70. https://doi.org/10.1016/j.marpolbul.2017.02.006.

Cha, J., Hong, S., Kim, J., Lee, J., Yoon, S.J., Lee, S., Moon, H.-B., Shin, K.-H., Hur, J., Giesy, J.P., Khim, J.S., 2019. Major AhR-active chemicals in sediments of Lake Sihwa, South Korea: application of effect-directed analysis combined with full-scan screening analysis. Environ. Int. 133, 105199 https://doi.org/10.1016/j.envint.2019.105199.

Gallo, A., Guida, M., Armiento, G., Siciliano, A., Mormile, N., Carraturo, F., Pellegrini, D., Morroni, L., Tosti, E., Ferrante, M.I., Montresor, M., Molisso, F., Sacchi, M., Danovaro, R., Lofrano, G., Libralato, G., 2020. Species-specific sensitivity of three microalgae to sediment elutriates. Mar. Environ. Res. 156, 104901 https://doi.org/10.1016/j.marenvres.2020.104901.

Gómez-Ramos, M.M., García-Valcárcel, A.I., Tadeo, J.L., Fernández-Alba, A.R., Hernando, M.D., 2016. Screening of environmental contaminants in honey bee wax comb using gas chromatography–high-resolution time-of-flight mass spectrometry. Environ. Sci. Pollut. Res. 23, 4609–4620. https://doi.org/10.1007/s11356-015-5667-0.

Hong, S., Lee, S., Choi, K., Kim, G.B., Ha, S.Y., Kwon, B.-O., Ryu, J., Yim, U.H., Shim, W. J., Jung, J., Giesy, J.P., Khim, J.S., 2015. Effect-directed analysis and mixture effects of AhR-active PAHs in crude oil and coastal sediments contaminated by the Hebei Spirit oil spill. Environ. Pollut. 199, 110–118. https://doi.org/10.1016/j.envpol.2015.01.009.

Kara, G.K., Rahimi, J., Niksefat, M., Taheri-Ledari, R., Rabbani, M., Maleki, A., 2020. Preparation and characterization of perlite/V_2O_5 nano-spheres via a novel green method: applied for oxidation of benzyl alcohol derivatives. Mater. Chem. Phys. 250, 122991 https://doi.org/10.1016/j.matchemphys.2020.122991.

Kim, J., Hong, S., Cha, J., Lee, J., Kim, T., Lee, S., Moon, H.-B., Shin, K.-H., Hur, J., Lee, J.-S., Giesy, J.P., Khim, J.S., 2019. Newly identified AhR-active compounds in the sediments of an industrial area using effect-directed analysis. Environ. Sci. Technol. 53, 10043–10052. https://doi.org/10.1021/acs.est.9b02166.

Kim, S., Lee, S., Kim, C., Liu, X., Seo, J., Jung, H., Ji, K., Hong, S., Park, J., Khim, J.S., Yoon, S., Lee, W., Park, J., Choi, K., 2014. In vitro and in vivo toxicities of sediment and surface water in an area near a major steel industry of Korea: endocrine disruption, reproduction, or survival effects combined with instrumental analysis. Sci. Total Environ. 470–471, 1509–1516. https://doi.org/10.1016/j.scitotenv.2013.08.010.

Koh, C.H., Khim, J.S., Kannan, K., Villeneuve, D.L., Senthilkumar, K., Giesy, J.P., 2004. Polychlorinated dibenzo-p-dioxins (PCDDs), dibenzofurans (PCDFs), biphenyls (PCBs), and polycyclic aromatic hydrocarbons (PAHs) and 2,3,7,8-TCDD equivalents (TEQs) in sediment from the Hyeongsan River, Korea. Environ. Pollut. 132, 489–501. https://doi.org/10.1016/j.envpol.2004.05.001.

Koh, C.-H., Khim, J.S., Villeneuve, D.L., Kannan, K., Giesy, J.P., 2006. Characterization of trace organic contaminants in marine sediment from Yeongil Bay, Korea: 1. Instrumental analyses. Environ. Pollut. 142, 39–47. https://doi.org/10.1016/j.envpol.2005.09.005.

Kwon, H.-C., Kwon, J.-H., 2012. Measuring aqueous solubility in the presence of small cosolvent volume fractions by passive dosing. Environ. Sci. Technol. 46, 12550–12556. https://doi.org/10.1021/es3035363.

Lee, J., Hong, S., Kim, T., Lee, C., An, S.-A., Kwon, B.-O., Lee, S., Moon, H.-B., Giesy, J.P., Khim, J.S., 2020. Multiple bioassays and targeted and nontargeted analyses to characterize potential toxicological effects associated with sediments of Masan Bay: Focusing on AhR-mediated potency. Environ. Sci. Technol. 54, 4443–4454. https://doi.org/10.1021/acs.est.9b07390.

Machado, M.D., Soares, E.V., 2019. Impact of erythromycin on a non-target organism: Cellular effects on the freshwater microalga *Pseudokirchneriella subcapitata*. Aquat. Toxicol. 208, 179–186. https://doi.org/10.1016/j.aquatox.2019.01.014.

Magnusson, M., Heimann, K., Negri, A.P., 2008. Comparative effects of herbicides on photosynthesis and growth of tropical estuarine microalgae. Mar. Pollut. Bull. 56, 1545–1552. https://doi.org/10.1016/j.marpolbul.2008.05.023.

Maleki, A., 2018. Green oxidation protocol: Selective conversions of alcohols and alkenes to aldehydes, ketones and epoxides by using a new multiwall carbon nanotube-based hybrid nanocatalyst via ultrasound irradiation. Ultrason. Sonochem. 40, 460–464. https://doi.org/10.1016/j.ultsonch.2017.07.020.

Maleki, A., Rahimi, R., Maleki, S., 2016. Efficient oxidation and epoxidation using a chromium(VI)-based magnetic nanocomposite. Environ. Chem. Lett. 14, 195–199. https://doi.org/10.1007/s10311-016-0558-2.

Marsili, R., 2001. Analysis of volatile compounds in the headspace of rice using SPMEGCMS. In: Marsili, R. (Ed.), Flavor, Fragrance, and Odor Analysis. Marcel Dekker Inc, New York, NY, pp. 229–248.

Mayo-Bean, K., Moran, K., Meylan, B., Ranslow, P., 2012. Methodology document for the ecological structure-activity relationship model (ECOSAR) class program. US-EPA, Washington DC.

Moore, D.R.J., Breton, R.L., MacDonald, D.B., 2003. A comparison of model performance for six quantitative structure-activity relationship packages that predict acute toxicity to fish. Environ. Toxicol. Chem. 22, 1799–1809. https://doi.org/10.1897/00-361.

Mosser, J.L., Fisher, N.S., Teng, T.-C., Wurster, C.F., 1972. Polychlorinated biphenyls: toxicity to certain phytoplankters. Science 175, 191–192. https://doi.org/10.1126/science.175.4018.191.

Niehus, N.C., Floeter, C., Hollert, H., Witt, G., 2018. Miniaturised marine algae test with polycyclic aromatic hydrocarbons – comparing equilibrium passive dosing and nominal spiking. Aquat. Toxicol. 198, 190–197. https://doi.org/10.1016/j.aquatox.2018.03.002.

Okumura, Y., Koayama, J., Uno, S., 2003. The relationship between logPow and molecular weight of polycyclic aromatic hydrocarbons and EC50 values of marine microalgae. La Mer 41, 182–191.

Olsen, R.O., Hess-Erga, O.K., Larsen, A., Hoffmann, F., Thuestad, G., Hoell, I.A., 2016. Dual staining with CFDA-AM and SYTOX blue in flow cytometry analysis of UV-irradiated Tetraselmis suecica to evaluate vitality. Aquat. Biol. 25, 39–52. https://doi.org/10.3354/ab00662.

Oros, D.R., Simoneit, B.R.T., 2000. Identification and emission rates of molecular tracers in coal smoke particulate matter. Fuel 79, 515–536. https://doi.org/10.1016/S0016-2361(99)00153-2.

Othman, H.B., Leboulanger, C., Le Floc'h, E., Hadj Mabrouk, H., Sakka Hlaili, A.,, 2012. Toxicity of benz[a]anthracene and fluoranthene to marine phytoplankton in culture: does cell size really matter? J. Hazard. Mater. 243, 204–211. https://doi.org/10.1016/j.jhazmat.2012.10.020.

Power, E.A., Munkittrick, K.R., Chapman, P.M., 1991. An ecological impact assessment framework for decision-making related to sediment quality. In: Mayes, M.A., Barron, M.G. (Eds.), Aquatic Toxicology and Risk Assessment. ASTM International, West Conshohocken, PA, pp. 48–64. ⟨https://www.astm.org/DIGITAL_LIBRARY/STP/PAGES/STP23563S.htm⟩.

Prado, R., Rioboo, C., Herrero, C., Cid, Á., 2011. Characterization of cell response in *Chlamydomonas moewusii* cultures exposed to the herbicide paraquat: induction of chlorosis. Aquat. Toxicol. 102, 10–17. https://doi.org/10.1016/j.aquatox.2010.12.013.

Prado, R., Rioboo, C., Herrero, C., Suárez-Bregua, P., Cid, Á., 2012. Flow cytometric analysis to evaluate physiological alterations in herbicide-exposed *Chlamydomonas moewusii* cells. Ecotoxicology 21, 409–420. https://doi.org/10.1007/s10646-011-0801-3.

Prato, E., Parlapiano, I., Biandolino, F., 2012. Evaluation of a bioassays battery for ecotoxicological screening of marine sediments from Ionian Sea (Mediterranea Sea, Southern Italy). Environ. Monit. Assess. 184, 5225–5238. https://doi.org/10.1007/s10661-011-2335-9.

Radix, P., Léonard, M., Papantoniou, C., Roman, G., Saouter, E., Gallotti-Schmitt, S., Thiébaud, H., Vasseur, P., 2000. Comparison of four chronic toxicity tests using algae, bacteria, and invertebrates assessed with sixteen chemicals. Ecotoxicol. Environ. Saf. 47, 186–194. https://doi.org/10.1006/eesa.2000.1966.

Rahimi, J., Taheri-Ledari, R., Niksefat, M., Maleki, A., 2020. Enhanced reduction of nitrobenzene derivatives: effective strategy executed by Fe_3O_4/PVA-10%Ag as a versatile hybrid nanocatalyst. Catal. Commun. 134, 105850 https://doi.org/10.1016/j.catcom.2019.105850.

Schwab, K., Altenburger, R., Varel, U.L.-V., Streck, G., Brack, W., 2009. Effect-directed analysis of sediment-associated algal toxicants at selected hot spots in the River Elbe

basin with a special focus on bioaccessibility. Environ. Toxicol. Chem. 28, 1506–1517. https://doi.org/10.1897/08-340.1.

Segovia, M., Berges, J.A., 2009. Inhibition of caspase-Like activities prevents the appearance of reactive oxygen species and dark-induced apoptosis in the unicullular chlorophyte *Dunaliella tertiolecta*. J. Phycol. 45, 1116–1126. https://doi.org/10.1111/j.1529-8817.2009.00733.x.

Sjollema, S.B., MartínezGarcía, G., van der Geest, H.G., Kraak, M.H.S., Booij, P., Vethaak, A.D., Admiraal, W., 2014. Hazard and risk of herbicides for marine microalgae. Environ. Pollut. 187, 106–111. https://doi.org/10.1016/j.envpol.2013.12.019.

Smital, T., Terzic, S., Zaja, R., Senta, I., Pivcevic, B., Popovic, M., Mikac, I., Tollefsen, K. E., Thomas, K.V., Ahel, M., 2011. Assessment of toxicological profiles of the municipal wastewater effluents using chemical analyses and bioassays. Ecotoxicol. Environ. Saf. 74, 844–851. https://doi.org/10.1016/j.ecoenv.2010.11.010.

Smith, K.E.C., Oostingh, G.J., Mayer, P., 2010. Passive dosing for producing defined and constant exposure of hydrophobic organic compounds during in vitro toxicity tests. Chem. Res. Toxicol. 23, 55–65. https://doi.org/10.1021/tx900274j.

Tang, J.Y.M., Aryal, R., Deletic, A., Gernjak, W., Glenn, E., McCarthy, D., Escher, B.I., 2013. Toxicity characterization of urban stormwater with bioanalytical tools. Water Res. 47, 5594–5606. https://doi.org/10.1016/j.watres.2013.06.037.

Tato, T., Salgueiro-González, N., León, V.M., González, S., Beiras, R., 2018. Ecotoxicological evaluation of the risk posed by bisphenol A, triclosan, and 4-nonylphenol in coastal waters using early life stages of marine organisms (*Isochrysis galbana*, *Mytilus galloprovincialis*, *Paracentrotus lividus*, and *Acartia clausi*). Environ. Pollut. 232, 173–182. https://doi.org/10.1016/j.envpol.2017.09.031.

USFDA, 2016. Safety and effectiveness of consumer antiseptics; Topical antimicrobial drug products for over-the-counter human use, in: Food and Drug Administration, New Hampshire, pp. 61106–61130. ⟨https://www.federalregister.gov/documents/2016/09/06/2016–21337/safety-and-effectiveness-of-consumer-antiseptics-topical-antimicrobial-drug-products-for⟩.

Weiner, J.A., DeLorenzo, M.E., Fulton, M.H., 2004. Relationship between uptake capacity and differential toxicity of the herbicide atrazine in selected microalgal species. Aquat. Toxicol. 68, 121–128. https://doi.org/10.1016/j.aquatox.2004.03.004.

Xue, Q., Wang, R., Xu, W., Wang, J., Tan, L., 2018. The stresses of allelochemicals isolated from culture solution of diatom *Phaeodactylum tricornutum* Bohlin on growth and physiology of two marine algae. Aquat. Toxicol. 205, 51–57. https://doi.org/10.1016/j.aquatox.2018.10.004.

Zhao, X.-Y., Zong, Z.-M., Cao, J.-P., Ma, Y.-M., Han, L., Liu, G.-F., Zhao, W., Li, W.-Y., Xie, K.-C., Bai, X.-F., Wei, X.-Y., 2008. Difference in chemical composition of carbon disulfide-extractable fraction between vitrinite and inertinite from Shenfu-Dongsheng and Pingshuo coals. Fuel 87, 565–575. https://doi.org/10.1016/j.fuel.2007.02.021.

Zheng, Q., Zhang, Y., Wahyudiono, Fouquet, T., Zeng, X., Kanda, H., Goto, M., 2020. Room-temperature extraction of direct coal liquefaction residue by liquefied dimethyl ether. Fuel 262, 116528. https://doi.org/10.1016/j.fuel.2019.116528.

Zhuravel, E., Markina, Z., Aizdaicher, N., 2009. Growth and physiological state of the microalgae Phaeodactylum tricornutum Bohlin (Bacillariophyta) in the water taken from peter the Great Bay. Ocean Sci. J. 44, 173–179. https://doi.org/10.1007/s12601-009-0015-2.

<Journal of Hazardous Materials>

Supplementary materials for

Identification of potential toxicants in sediments from an industrialized area in Pohang, South Korea: Application of a cell viability assay of microalgae using flow cytometry

Seong-Ah An, Seongjin Hong*, Junghyun Lee, Jihyun Cha, Sunggyu Lee, Hyo-Bang Moon, John P. Giesy, Jong Seong Khim*

This PDF file includes:

Number of pages: 29

Number of Supplementary Tables: 16, Tables S1 to S16

Number of Supplementary Figures: 3, Figs. S1 to S3

References

***Corresponding Authors.**

E-mail addresses: hongseongjin@cnu.ac.kr (S. Hong), jskocean@snu.ac.kr (J.S. Khim).

Supplementary Tables

Table S1. Reverse phase (RP)-HPLC conditions for fractionation of silica gel column fractions (Hong et al., 2016).

Instrument	Agilent 1260 HPLC system (Preparative scale) 1260 Multiple wavelength detector
Column	PrepHT XDB-C18 reverse phase column (250 mm × 21.2 mm × 7 μm)
Mobile phase	A: Water, B: Methanol
Flow rate	10 mL $min.^{-1}$
Injection volume	1 mL
Mobile phase gradient	40% A (0 min.) → 40–0% A (0–40 min.) → 0% A (40–60 min.) → 0–40% A (60–62 min.) → 40% A (62–70 min.) 60% B (0 min.) → 60–100% B (0–40 min.) → 100% B (40–60 min.) → 100–60% B (60–62 min.) → 60% B (62–70 min.)
Test standards	34 polychlorinated biphenyls 16 polycyclic aromatic hydrocarbons 7 alkylphenols 5 phthalates
Fractions collected times	

RP-HPLC Sub-fraction	Starting –End sampling time (min.)	Log Kow
1	3.11 – 6.35	< 1
2	6.35 – 12.83	1 – 2
3	12.83 – 19.32	2 – 3
4	19.32 – 25.80	3 – 4
5	25.80 – 32.29	4 – 5
6	32.29 – 38.78	5 – 6
7	38.78 – 45.26	6 – 7
8	45.26 – 51.70	7 – 8
9	51.70 – 58.23	8 – 9
10	58.23 – 64.72	> 9

Table S2. Culture conditions of the three microalgae and test conditions of each microalgal species for which the cell viability of algal cells was measured using flow cytometry.

Scientific name	***Dunaliella tertiolecta***	***Isochrysis galbana***	***Phaeodactylum tricornutum***
Class	Chlorophyceae	Prymnesiophyceae	Bacillariophyceae
Cell size	6−14 μm	5−6 μm	5−6 μm × 10−14 μm
Culture condition	f/2 medium + autoclaved seawater (121 ℃), 20 ℃, 12:12 (Light : Dark), 100 rpm		
Initial cell density	7×10^4 cells mL^{-1}	6×10^4 cells mL^{-1}	3×10^4 cells mL^{-1}
Staining protocol	Double staining	Double staining	Single staining
Dye	FDA (fluorescein diacetate) + SYTOX blue	FDA + SYTOX blue	FDA, PI (propidium iodide)
Ex/Em (nm)	488/530, 444/480	488/530, 444/480	488/530, 488/582
Endpoint	Growth inhibition (72 h) Esterase activity (FDA) Cell membrane intensity (SYTOX blue) Chlorophyll *a* Cell size (FS) Intracellular complexity (SS)	Growth inhibition (72 h) Esterase activity (FDA) Cell membrane intensity (SYTOX blue) Chlorophyll *a* Cell size (FS) Intracellular complexity (SS)	Growth inhibition (72 h) Esterase activity (FDA) Cell membrane intensity (PI) Chlorophyll *a* Cell size (FS) Intracellular complexity (SS)

Table S3. Overview of the quadrants (Q1−Q4) in response to elevated (+) and low (−) fluorescence intensity when cells were stained with FDA and SYTOX blue (Olsen et al., 2016).

Quadrant	FDA	SYTOX blue	Physiological characteristics	Vitality
Q1	+	−	Esterase active; membrane intact	Healthy
Q2	+	+	Esterase active; membrane damaged	Severely damaged
Q3	−	−	Esterase inactive; membrane intact or DNA/RNA degraded	Severely damaged
Q4	−	+	Esterase inactive; membrane damaged	Stressed

Table S4. Concentration of each compound in the sediments of Yeongil Bay.

Chemical class	Compounds (ng g^{-1} dry mass)	Abb.[a]	Organic extracts of sediments					
			S1	S2	S3	S4	S5	S6
PAHs	Acenaphthene	Ace	6100[b]	< DL[c]	< DL	< DL	< DL	< DL
	Acenaphthylene	Acl	1200	< DL	< DL	< DL	3.1	< DL
	Fluorene	Flu	19000	2.2	< DL	< DL	< DL	< DL
	Phenanthrene	Phe	56000	22	3.4	4.2	15	< DL
	Antracene	Ant	11000	13	< DL	< DL	< DL	< DL
	Fluoranthene	Fl	42000	< DL	4.5	6.8	20	< DL
	Pyrene	Py	24000	67	5.4	6.2	20	< DL
	Benzo[*a*]anthracene	BaA	13000	24	< DL	< DL	< DL	< DL
	Chrysene	Chr	12000	22	0.73	1.8	8.8	< DL
	Benzo[*b*]fluoranthene	BbF	19000	25	< DL	< DL	4.3	< DL
	Benzo[*k*]fluoranthene	BkF	2300	5.1	< DL	< DL	< DL	< DL
	Benzo[*a*]pyrene	BaP	7000	9.1	3.3	1.6	8.1	< DL
	Indeno[*1,2,3-cd*]pyrene	IcdP	1400	4.1	< DL	< DL	4.8	< DL
	Dibenz[*a,h*]anthracene	DbahA	2200	< DL	< DL	< DL	< DL	< DL
	Benzo[*g,h,i*]perylene	BghiP	4800	5.6	< DL	< DL	7.3	< DL
SOs	1,3-Diphenylproane	SD1	6.3	1.6	< DL	< DL	< DL	1.7
	2,4-Diphenyl-1-butene	SD3	98	56	52	26	36	66
	4,6-Triphenyl-1-hexene	ST1	16	12	12	12	18	12
	1,3,5-Triphenylcyclohexane (isomer mix)	ST6	25	< DL	< DL	< DL	< DL	< DL
APs	4-*tert*-Octylphenol	t-OP	49	0.29	< DL	0.19	0.77	0.075
	Nonylphenol	NPs	13	0.43	< DL	0.072	0.26	0.018
	4-*tert*-Octylphenol-monoethoxylate	t-OP1EO	5.2	0.40	0.40	0.35	0.35	0.40
	Nonylphenol-monoethoxylates	NP1EOs	11	0.23	< DL	< DL	0.086	0.086
	Bisphenol A	BPA	14	1.1	2.6	1.4	8.0	51
	4-*tert*-Octylphenol-diethoxylate	t-OP2EO	2.9	< DL	< DL	< DL	< DL	< DL
	Nonylphenol-diethoxylates	NP2EOs	2.9	< DL	< DL	< DL	< DL	< DL

[a] Abb.: Abbreviations.
[b]: Shade indicated of exceed PEL values (CCME, 2002).
[c] < DL: Below detection limits.

Table S5. GC-MSD conditions for the targeted analysis of polycyclic aromatic hydrocarbons (PAHs), styrene oligomers (SOs), and alkylphenols (APs).

Instrument		GC : Agilent 7890B MS : Agilent 5977B MSD
Column		DB-5ms (30 m × 250 μm i.d. × 0.25 μm film)
Carrier gas		He
Flow rate		1.0 mL min^{-1}
Injection mode		Splitless
Injection volume		1 μL
Ionization mode		EI mode (70 eV)
Ion source temperature		230 °C
Acquisition mode		SIM mode
Oven temperature program	**PAHs**	60 °C (hold 2 min.) → 6 °C $min.^{-1}$ to 300 °C (hold 13 min.)
	SOs	60 °C (hold 2 min.) → 6 °C $min.^{-1}$ to 300 °C (hold 13 min.)
	APs	10 °C $min.^{-1}$ to 100 °C → 20 °C $min.^{-1}$ to 300 °C (hold 6 min.)

Table S6. GC-QTOFMS conditions for full-scan screening analysis.

Instrument	GC : Agilent 7890B QTOFMS : Agilent 7200
Samples	S1 (Gumu Creek) F2.7 RP-HPLC fractions
Column	DB-5MS UI (30 m × 0.25 μm i.d. × 0.25 μm film)
Carrier gas	He
Flow rate	1.2 mL $min.^{-1}$
Injection volume	2 μL
Mass range	50−600 *m/z*
Ion source temperature	230 ℃
Ionization mode	EI mode (70 eV)
Software	Qualitative analysis B.07.01 MassHunter Quantitative analysis Unknown analysis NIST Library (ver. 2014)
Identification criteria for potential algal toxicants	Minimum number of ion peaks > 5 Peak shape quality > 60% Matching factor scores of ≥ 90 - Matching factor score (the accurate mass pattern match score) = Contribution of Mass Abundance Score, Mass Accuracy Score, Mass Spacing Score - Mass Abundance Score records how well the abundance pattern of the measured isotope cluster compared with values predicted from the proposed formula - Mass Accuracy Score records how well the measured mass (or m/z) compared with the value predicted from the proposed formula - Mass Spacing Score records how the m/z spacing between the lowest m/z ion and the A+1 and A+2 ions compared with the values predicted from the proposed formula

Table S7. The review of toxicity evaluation of toxic substances using microalgal bioassays.

Matrix		Microalgae species	Endpoints	EDA	Identified or potential toxicants	Reference
Standard	Cu	*Phaeodactylum tricornutum*	Cell membrane intensity Peroxidase activity Membrane potential	-	-	Cid et al. (1996)
	Cu	*Dunaliella tertiolecta* *Phaeodactylum tricornutum* *Pseudokerchnerella subcapitata* *Chlorella* sp.	Growth rate Esterase activity Chlorophyll a fluorescence Membrane potential Cell size Intracellular complexity	-	-	Franklin et al. (2001)
	Perfluorobutanoic sulfonate Perfluorooctane sulfonate Perfluorohexanoic acid Perfluorooctanoic acid Perfluorododecanoic acid Perfluorotetradecanoic acid	*Scenedesmus obliquus*	Growth inhibition Esterase activity Cell membrane intensity Chlorophyll *a* fluorescence Mitochondrial membrane potential	-	-	Liu et al. (2008)
	Paraquat	*Chlamydomonas moewusii*	Esterase activity Chlorophyll *a* fluorescence Cell size Intracellular complexity Chlorophyll contents	-	-	Prado et al. (2011)
	Florfenicol	*Skeletonema costatum*	Growth inhibition Esterase activity Reactive oxygen species contents Intracellular pH Cell size PSII inhibition	-	-	Liu et al. (2012)
	Paraquat	*Chlamydomonas moewusii*	Esterase activity Chlorophyll *a* fluorescence Reactive oxygen species contents Membrane potential Protein contents	-	-	Prado et al. (2012)

Table S7. (continued).

Matrix		Microalgae species	Endpoints	EDA	Identified or potential toxicants	Reference
Standard	Paraquat	*Chlamydomonas moewusii*	Esterase activity Cell membrane intensity Chlorophyll a fluorescence Reactive oxygen species contents Membrane potential Mitochondrial membrane potential Intracellular free calcium Intracellular pH Cell size Intracellular complexity	-	-	Prado et al. (2012)
	Paraquat	*Chlamydomonas reinhardtii*	Growh inhibition Esterase activity Reactive oxygen species contents Oxidative DNA damage Mitochondrial membrane potential DNA contents Comet assay	-	-	Esperanza et al. (2015)
	Cd, Cr, Cu, Zn	*Pseudokirchneriella subcapitata*	Growh inhibition Esterase activity Cell membrane intensity Mitochondrial membrane potential Chlorophyll content PSII inhibition	-	-	Machado et al. (2015)
	Graphene oxide	*Pseudokirchneriella subcapitata*	Growth inhibition Esterase activity Cell membrane intensity Reactive oxygen species contents	-	-	Nogueira et al. (2015)

Table S7. (continued).

Matrix		Microalgae species	Endpoints	EDA	Identified or potential toxicants	Reference
Standard	Diuron Isoproturon Metazachlor Chlorpyrifos-methyl Azoxystrobin Quinoxyfen Spiroxamine	*Tisochrysis lutea* *Skeletonema marinoi*	Growh inhibition Esterase activity Reactive oxygen species contents Superoxide anion content Membrane potential Lipid contents PSII inhibition	-	-	Dupraz et al. (2019)
	Benzophenone-3 Benzophenone-4	*Chlamydomonas reinhardtii*	Growth inhibition Esterase activity Cell membrane intensity Chlorophyll *a* fluorescence Reactive oxygen species contents Membrane potential Mitochondrial-membrane potential Intracellular pH	-	-	Esperanza et al. (2019)
Environmental samples	Sediments	*Scenedesmus vacuolatus*	Growth inhibition	O	-	Grote et al. (2005)
	Sediments Water Porewater	*Pseudokirchneriella subcapitata*	Growth inhibition	-	-	Källqvist et al. (2008)
	Sediments	*Scenedesmus vacuolatus*	Growth inhibition	O	-	Bandow et al. (2009a)
	Sediments	*Scenedesmus vacuolatus*	Growth inhibition	O	Triclosan 2-Methylanthraquinone Benz[*a*]anthrone Cyclopenta[*def*]phenanthren-4-one Benz[*c*]acridine Hexadecanol Palmetic acid Pentadecanol	Bandow et al. (2009b)

Table S7. (continued).

Matrix		Microalgae species	Endpoints	EDA	Identified or potential toxicants	Reference
Environmental samples	Sediments	*Scenedesmus vacuolatus*	Growth inhibition	O	7H-benzo[de]anthracen-7-one N-phenyl-2-naphthylamine	Schwab et al. (2009)
	Water	*Pseudokirchneriella subcapitata*	Growth inhibition PSII inhibition	-	-	Vermeirssen et al. (2010)
	Waste water	*Desmodesmus subspicatus*	Growth inhibition	-	-	Smital et al. (2011)
	Water	*Dunaliella tertiolecta*	PSII inhibition	O	Atrazine Diuron Irgarol Isoproturon Terbutryn Terbutylazine	Booij et al. (2014)
	Waste water	*Pseudokirchneriella subcapitata*	Growth inhibition	O	Terbutryn Terbuthylazine Prometryn, etc.	Tousova et al. (2018)
	Water	*Selenastrum capricornutum* *Pseudokirchneriella subcapitata* *Phaeodactylum tricornutum*	PSII inhibition	O	Terbutryn Atrazine Simazine Diuron	Riegraf et al. (2019)
	Bottled waters	*Pseudokirchneriella subcapitata*	Growth inhibition Esterase activity Cell membrane intensity Reactive oxygen species formation Mitochondrial-membrane potential Lipid peroxidation DNA contents Cell size Intracellular complexity Chlorophyll contents PSII inhibition	-	-	Almeida et al. (2019)

Table S7. (continued).

Matrix		Microalgae species	Endpoints	EDA	Identified or potential toxicants	Reference
Environmental samples	Water	*Pseudokirchneriella subcapitata* *Chlorella vulgaris*	Growth inhibition Esterase activity Cell membrane intensity Chlorophyll a autofluorescence Alkaline phosphatase activity	-	-	Gosset et al. (2019)
	Vehicle emitted particles	*Porphyridium purpureum* *Heterosigma akashiwo*	Esterase activity Cell membrane intensity Membrane potential	-	-	Pikula et al. (2019)
	Water	*Phaeodactylum tricornutum*	Growth inhibition	-	-	Moeris et al. (2019)
	Water	*Scenedesmus obliquus*	Growth inhibition, Chlorophyll contents Superoxide dismutase activity Algal macromolecules analysis Intracellular complexity	-	-	Cai et al. (2020)
	Sediments	*Isochrysis galbana* *Phaeodactylum tricornutum*	Growth inhibition Esterase activity Cell membrane intensity Chlorophyll a autofluorescence Cell size Intracellular complexity	O	Nonylphenols	Lee et al. (2020)
	Sediments	*Dunaliella tertiolecta* *Isochrysis galbana* *Phaeodactylum tricornutum*	Growth inhibition Esterase activity Cell membrane intensity Chlorophyll a autofluorescence Cell size Intracellular complexity	O	1-Phenylpyrene Dibenz[*a,c*]anthracene Picene, etc.	This study

Table S8. Results of exposed organic extracts and fractions on *Dunaliella tertiolecta* (Mean ± standard deviation).

Organic extracts and fractions			Growth inhibition	Cell viability				
				Esterase activity inhibition	Cell membrane damaged	Chl. *a*[a]	Cell size	Intracellular complexity
Raw extracts	S1		-95±1.4	14±5.4	1.4±1.2	3.5±1.1	2.2±0.61	-
	S2		-110±7.2	6.6±0.7	5.8±4.3	4.6±3.3	3.5±1.8	0.57±0.38
	S3		1.0±2.1	93±6.5	-	2.9±1.5	4.2±2.5	-
	S4		-61±7.5	-	-	1.2±2.4	2.6±1.3	-
	S5		0.7±2.5	97±1.2	-	4±0.47	2.8±0.63	0.11±0.39
	S6		-4.6±5.1	92±6.2	-	4.4±0.30	9.0±0.52	4.2±0.65
Silica gel fractions	S1	F1	-68±2.9	16±4.1	-	3.1±0.77	2.4±0.18	-
		F2	100	99±0.20	99±0.18	49±0.85	39±4.6	9.8±0.74
		F3	25	99±0.20	93±2.3	59±3.5	47±1.2	1.6±1.2
	S2	F1	-89±7.3	0.94±3.8	1.4±1.9	0.1±0.72	0.71±0.48	-
		F2	-28±7.4	3.5±3.8	5.8±2.5	0.33±0.55	0.78±0.33	-
		F3	-33±7.4	19±1.7	-	1.7±0.48	1.7±0.26	0.28±0.18
	S4	F1	-15±10	9.2±7.7	-	-	0.35±0.22	
		F2	-0.39±3.4	14±4.4	-	-	2.0±0.13	0.32±0.33
		F3	-28±4.8	20±2.9	5.4±2.2	-	2.2±0.83	0.28±0.58
RP-HPLC fractions	S1	F2.1	-55±31	-	-	-	-	-
		F2.2	-61±11	-	-	-	0.77±1.0	-
		F2.3	-26±7.8	-	-	-	0.6±0.78	-
		F2.4	-49±2.4	-	-	-	0.39±0.13	-
		F2.5	-48±3.1	11±0.66	2.6±6.1	2.6±3.2	1.8±0.82	-
		F2.6	100	95±0.13	97±0.51	40±5.1	4.5±0.65	1.5±1.3
		F2.7	18±20	75±5.4	97±0.60	20±2.0	4.4±1.1	0.37±0.58
		F2.8	-45±4.4	2.0±13	19±4.5	1.2±4.1	0.53±0.82	-
		F2.9	-86±12	-	-	-	-	-
		F2.10	-71±11	1.7±11	2.3±6.6	-	0.6±0.55	-
		F3.1	-27±10	6.0±0.73	2.3±0.71	-	-	-
		F3.2	-10±4.2	32±9.9		-	-	-
		F3.3	4.5±4.8	25±7.5	3.4±4.0	-	-	-
		F3.4	9.3	50±5.8		-	-	-
Distributed outside the control gate		F3.5	67	55±2.4	51±10	-	0.53±0.45	-
		F3.6	-4.6±4.4	43±17	17±11	-	-	-
		F3.7	-32±19	35±2.4	0.49±4.1	-	0.84±0.87	-
20−50%		F3.8	-16±4.8	25±3.4	-	-	-	-
50−80%		F3.9	-45±13	30±0.22	-	-	-	-
80−100%		F3.10	-32±10	50±12	-	-	-	-

[a] Chl. *a*: Chlorophyll *a*

Table S9. Results of exposed organic extracts and fractions on *Isochrysis galbana* (Mean ± standard deviation).

Organic extracts and fractions			Growth inhibition	Cell viability					
				Esterase activity inhibition	Cell membrane damaged	Chl. *a*[a]	Cell size		Intracellular complexity
							Increase	Decrease	
Raw extracts	S1		-3.3±3.1	35±12	-	-	-	-	-
	S2		-4.2±5.0	71±19	5.5±2.2	-	-	-	-
	S3		5.0±1.6	3.3±1.7	21±2.1	0.94±0.24	-	-	0.81±0.41
	S4		11±1.5	79±3.4	54±13	0.57±1.2	5.0±1.3	-10±1.3	3.8±1.1
	S5		9.1±0.59	41±12	22±1.4	-	3.3±3.6	-	0.99±2.0
	S6		0.50±2.2	0.46±7.0	29±4.2	0.03±0.05	0.31±0.26	-	0.74±0.50
Silica gel fractions	S1	F1	31	45±38	1.7±0.69	-	-	-	-
		F2	100	99	99	99	9.0	-44	34
		F3	100	100	99	99	13	-32	37
	S2	F1	4.9±5.0	13±6.6	19±2.0	-	-	-	-
		F2	-0.15	28±9.7	6.3±3.1	-	1.3±0.09	-	-
		F3	-5.2±5.0	48±4.4	5.3±1.2	-	2.5±0.58	-	0.67±0.75
	S4	F1	8.5±1.4	19±0.50	12±2.6	-	1.4±0.48	-	-
		F2	2.3±3.4	28±5.9	13±6.1	1.2±1.1	3.0±1.0	-	0.88±0.65
		F3	3.2±4.7	28±4.4	12±5.0	-	1.2±0.76	-	-
RP-HPLC fractions	S1	F2.1	-1.8±2.3	17±15	0.83±0.83	-	0.26±0.89	-	0.39±0.18
		F2.2	-3.8±7.1	11±2.6	0.43±1.2	-	1.1±1.5	-	0.98±0.60
		F2.3	-5.1	7.9±2.5	0.39±0.78	-	1.4±0.40	-	0.67±0.52
		F2.4	-5.9±8.7	9.6±1.8	-	-	-	-	0.49±0.30
		F2.5	3.6±3.6	12±2.9	-	0.24±0.35	-	-	0.53±1.0
		F2.6	100	89	73	82	11	-43	28
		F2.7	100	97	89	88	15	-37	43
		F2.8	100	57	68	9.3	1.4	-	1.9
		F2.9	17±11	12±3.0	2.7±2.3	-	-	-	-
		F2.10	1.0±4.4	-	-	-	-	-	-
		F3.1	-13±3.0	-	8.1±10	-	-	-	-
		F3.2	-14±4.8	-	1.8±1.2	-	-	-	-
		F3.3	-1.3±3.8	-	-	-	-	-	-
		F3.4	5.5±3.0	16±3.1	-	-	-	-	-
Distributed outside the control gate		F3.5	27±9.4	15±4.4	42±5.6	0.52±0.94	2.5±1.1	-	3.0±0.91
		F3.6	33±7.1	26±15	70±7.8	0.030±0.47	-	-	1.1±0.78
		F3.7	5.5±3.0	13±4.7	2.7±1.1	-	0.79±1.8	-	-
20–50%		F3.8	-0.59±6.4	5.5±2.7	1.1±2.5	-	1.6±3.3	-	-
50–80%		F3.9	-10±5.3	17±3.7	3.1±1.2	-	0.26±1.3	-	-
80–100%		F3.10	-16	1.3±3.1	-	-	-	-	-

[a] Chl. *a*: Chlorophyll *a*

Table S10. Results of exposed organic extracts and fractions on *Phaeodactylum tricornutum* (Mean ± standard deviation).

Organic extracts and fractions			Growth inhibition	Cell viability				
				Esterase activity inhibition	Cell membrane damaged	Chl. *a*[a]	Cell size	Intracellular complexity
Raw extracts	S1		19±1.6	-	24±0.31	3.9	1.8±0.06	-
	S2		40±4.9	-	3.7±0.01	-	0.45±0.02	-
	S3		5.9±0.47	99±0.31	0.82±0.11	-	-	0.29±0.74
	S4		21±7.0	23±0.12	5.6±0.02	0.55	1.7±0.03	-
	S5		-0.8±0.6	100±0.04	0.47±0.94	-	-	-
	S6		2.1±3.8	99±0.36	0.94±1.3	-	-	-
Silica gel fractions	S1	F1	34±5.1	-	1.1±0.03	1.8	0.71±0.17	-
		F2	100	-	-	-	-	-
		F3	100	-	-	-	-	-
	S2	F1	11±3.9	48±0.14	2.4±0.0485	-	0.64±0.01	-
		F2	3.5±2.7	30±0.04	1.4±0.07	0.74	0.19	-
		F3	5.0±3.6	40±0.04	1.7	1.5	0.26±0.01	-
	S4	F1	20±1.7	61±0.04	5.6	-	1.1±0.01	-
		F2	7.3±3.9	59	4.2	0.23	0.66	-
		F3	0.43±5.5	66	2.9	-	1.3	-
RP-HPLC fractions	S1	F2.1	5.3±2.2	-	-	0.27	0.41±0.05	1.1±0.44
		F2.2	7.5	0.63±0.49	-	0.29	0.15±0.01	-
		F2.3	5.3±3.0	0.21±0.13	-	0.59	0.98±0.06	2.3±0.72
		F2.4	-6.4±3.2	0.63±0.08	-	0.41	0.53±0.04	2.4±0.42
		F2.5	24±1.9	5.2±0.04	0.68±0.04	1.6	2.1±0.06	2.0±0.61
		F2.6	100	-	-	-	-	-
		F2.7	100	-50	-	0.66	1.4	0.61
		F2.8	7.7±3.9	-4.6±0.04	-	0.12	0.61±0.02	0.83±0.41
		F2.9	16±6.1	-13±0.03	-	0.34	0.47±0.02	0.86±0.32
		F2.10	8.6±5.1	-16±0.20	-	1.2	1.1±0.06	0.9±0.06
		F3.1	-2.7	-14±0.06	1.5	0.56	0.53±0.05	1.3±0.18
		F3.2	-4.3±1.7	-17±0.13	0.56	0.79	0.81±0.02	0.97±0.19
		F3.3	4.1±4.8	-16±0.02	0.23	0.51	0.46±0.07	2.00±0.38
		F3.4	8.6±5.1	-17±0.13	-	-	0.22±0.02	1.00±0.27
Distributed outside the control gate		F3.5	11±3.9	-22±0.22	-	0.2	0.36±0.05	0.46±0.22
		F3.6	10±5.8	-24±0.43	-	0.03	1±0.10	2.2±1.2
		F3.7	19±1.6	-38±0.12	-	0.34	1.1±0.16	1.2±1.8
20−50%		F3.8	4.1±4.8	-32±0.10	-	0.84	1.3±0.16	2.7±0.58
50−80%		F3.9	2.4±5.1	-33±0.16	2.6	0.95	0.61±0.09	1.7±0.21
80−100%		F3.10	3.5±5.6	-33±0.60	-	0.51	0.76±0.11	0.91±0.67

[a] Chl. *a*: Chlorophyll *a*

Table S11. Comparison of concentrations of PAHs in sediments of S1 and probable effect levels (PELs) (CCME, 2002).

Compounds	**Concentration (ng g^{-1} dry mass)**	**Probable effect levels (PELs)**	**Exceedance of PELs (times)**
Acenaphthene	1200	128	9.4
Acenaphthylene	6100	88.9	69
Fluorene	19000	144	132
Phenanthrene	56000	544	103
Antracene	11000	245	45
Fluoranthene	42000	1494	28
Pyrene	24000	1398	17
Benzo[*a*]anthracene	13000	693	19
Chrysene	12000	846	14
Benzo[*a*]pyrene	7000	763	9.2
Dibenz[*a,h*]anthracene	2200	135	16

Table S12. EC50 values of PAHs on each microalgal species reported in the previous studies.

Compounds	**Abbreviations.**	**EC50 (μg L^{-1})**		
		D. tertiolecta	***I. galbana***	***P. tricornutum***
Acenaphthylene	Ace	-	-	1800[a]
Fluorene	Flu	1100[b]	110[b]	-
Phenanthrene	Phe	-	140[b]	150[c]
Anthracene	Ant	-	65[c]	120[d]
Fluoranthene	Fl	390 [e]	140[e]	100[c], 370[e]
Pyrene	Py	-	-	120[c]
Benz[*a*]anthracene	BaA	790[e]	260[e]	-
Benzo[*a*]pyrene	BaP	-	88[d]	-

[a]: Niehus et al. (2018).
[b]: Okumura et al. (2003).
[c]: Wang et al. (2008).
[d]: Huang et al. (2000).
[e]: Othman et al. (2012).

Table S13. Predicted algal toxicity of PAHs, SOs, and APs using ECOSAR.

Compound classes	Eluted fraction	Compounds (ng g^{-1} dry mass)	Abb.[a]	Predicted toxicity (EC50, mg L^{-1})
PAHs	F2.4	Acenaphthene	Ace	1.7
	F2.5	Acenaphthylene	Acl	2.4
		Fluorene	Flu	2.3[b]
		Phenanthrene	Phe	1.5[b]
		Antracene	Ant	1.5[b]
	F2.6	Fluoranthene	Fl	0.66[b]
		Pyrene	Py	0.66[b]
		Benzo[*a*]anthracene	BaA	0.29[b]
		Chrysene	Chr	0.29[b]
	F2.7	Benzo[*b*]fluoranthene	BbF	0.13[b]
		Benzo[*k*]fluoranthene	BkF	0.13[b]
		Benzo[*a*]pyrene	BaP	0.13[b]
		Indeno[*1,2,3-cd*]pyrene	IcdP	0.054[b]
		Dibenz[*a,h*]anthracene	DbahA	0.054[b]
		Benzo[*g,h,i*]perylene	BghiP	0.054[b]
SOs	F2.6	1,3-Diphenylpropane	SD1	0.40
		cis-1,2-Diphenylcyclobutane	SD2	0.40
		2,4-Diphenyl-1-butene	SD3	0.22
		trans-1,2-Diphenylcyclobutane	SD4	0.29
	F2.7	2,4,6-Triphenyl-1-hexene	ST1	0.0050
		1e-Phenyl-4e-(1-phenylethyl)-tetralin	ST2	0.014[b]
		1a-Phenyl-4e-(1-phenylethyl)-tetralin	ST3	0.014[b]
		1a-Phenyl-4a-(1-phenylethyl)-tetralin	ST4	0.014[b]
		1e-Phenyl-4a-(1-phenylethyl)-tetralin	ST5	0.014[b]
		1,3,5-Triphenylcyclohexane (isomer mix)	ST6	0.070
APs	F3.4	4-*tert*-Octylphenol	*t*-OP	1.6
		Nonylphenols	NPs	0.13
	F3.5	4-*tert*-Octylphenol-mono-ethoxylate	*t*-OP1EO	0.76
		Nonylphenol-mono-ethoxylates	NP1EOs	0.31
	F3.6	Bisphenol A	BPA	1.3
		4-*tert*-Octylphenol-di-ethoxylate	*t*-OP2EO	1.7
		Nonylphenol-di-ethoxylates	NP2EOs	0.56

[a] Abb.: Abbreviations.
[b]: Exceed value of predicted water solubility using ECOSAR.

Table S14. Concentration of PAHs in the artificial mixture based on targeted analysis in the F2.7 fraction.

Compounds	**Abbreviations**	**mg L^{-1}**
Benzo[*b*]fluoranthene	BbF	18
Benzo[*k*]fluoranthene	BkF	8.7
Benzo[*a*]pyrene	BaP	17
Indeno[*1,2,3-cd*]pyrene	IcdP	5.7
Dibenz[*a,h*]anthracene	DbahA	2.8
Benzo[*g,h,i*]perylene	BghiP	3.2

Table S15. Results of the exposed artificial mixture on the three microalgal species.

Microalgae species	Growth inhibition	Cell viability					
		Esterase activity inhibition	Cell membrane damaged	Chl. *a*[a]	Cell size		Intracellular complexity
					Increase	Decrease	
D. tertiolecta	-22	29±0.66[b]	-	-	-	-	-
I. galbana	98[c]	74[d]	98	46	-	-26	9.5
P. tricornutum	7.4	-42±0.11	-	0.27	1.1±0.045	-	0.66±1.0

[a]: Chlorophyll *a*.
[b]: Yellow Shade indicated that 20−50% cells were distributed outside the control gate.
[c]: Red Shade indicated that 80−100% cells were distributed outside the control gate.
[d]: Orange Shade indicated that 50−80% cells were distributed outside the control gate.

Table S16. List of predicted algal toxicant compounds in the F2.7 fractions using ECOSAR.

CAS#	Compound Name	Formula	Predicted toxicity (EC50, mg L^{-1})	Uses/origins	Reference
604-53-5	1,1'-Binaphthalene	$C_{20}H_{14}$	0.126[a]		
4325-74-0	1,2'-Binaphthalene	$C_{20}H_{14}$	0.126[a]		
612-78-2	2,3'-Binaphthalene	$C_{20}H_{14}$	0.126[a]		
3351-28-8	1-Methylchrysene	$C_{19}H_{14}$	0.129[a]	Wood combustion	Hedberg et al. (2002)
3351-31-3	3-Methylchrysene	$C_{19}H_{14}$	0.129[a]	Wood combustion	Hedberg et al. (2002)
93870-57-6	1-Methyl-4-p-tolylnaphthalene	$C_{18}H_{16}$	0.132		
3674-73-5	2,3,5-Trimethylphenanthrene	$C_{17}H_{16}$	0.133[a]		
19353-76-5	7-Ethyl-1-methylphenanthrene	$C_{17}H_{16}$	0.146[a]		
2091-92-1	5,6-Dihydrochrysene	$C_{18}H_{14}$	0.156[a]		
4389-09-07	5,6-dihydro-4H-Benz[*de*]anthracene	$C_{17}H_{14}$	0.173[a]	Byproducts of coal liquefaction	Zheng et al. (2020)
217-59-4	Triphenylene	$C_{18}H_{12}$	0.29[a]	Components of coal	Zhao et al. (2008)
84-15-1	*o*-Terthenyl	$C_{18}H_{14}$	0.292		
3442-78-2	2-Methylpyrene	$C_{17}H_{12}$	0.293[a]	Charcoal combustion	Dyremark et al. (1995)
483-87-4	1,7-Dimethylphenanthrene	$C_{16}H_{14}$	0.298[a]	Wood combustion	Benner et al. (1995)
3674-66-6	2,5-Dimethylphenanthrene	$C_{16}H_{14}$	0.298[a]	Components of wood tar	Egenberg et al. (2002)
2717-39-7	1,4,5,8-Tetramethylnaphthalene	$C_{14}H_{16}$	0.303		
2000157-19-2	2,4,6,8-Tetramethylazulene	$C_{14}H_{16}$	0.303		
3976-35-0	2,4,6-Trimethylbiphenyl	$C_{15}H_{16}$	0.303		
31317-19-8	2,7-Dimethyldibenzothiophene	$C_{14}H_{12}S$	0.335[a]		
241-35-0	Indolo[*2,3-b*]carbazole	$C_{18}H_{12}N_2$	0.341		
205-43-6	Benzo[*b*]naphtho[*1,2-d*]thiophene	$C_{16}H_{10}S$	0.396[a]	Components of oil	Grimmer et al. (1983)
490-65-3	1-Methyl-7-(1-methylethyl)-naphthalene	$C_{14}H_{16}$	0.408	Wood combustion	Ramdahl (1983)
613-59-2	2-Benzylnaphthalene	$C_{17}H_{14}$	0.469		
612-94-2	2-Phenylnaphthalene	$C_{16}H_{12}$	0.662	Used to produce liquid crystals	Funahashi and Hanna (1997)
613-12-7	2-Methylanthracene	$C_{15}H_{12}$	0.665[a]	Combustion	Safarik and Strausz (1997)
883-20-5	9-Methyphenanthrene	$C_{15}H_{12}$	0.665[a]	Wood combustion	Schauer et al. (2001)
2245-38-7	1,6,7-Trimethyl-naphthalene	$C_{13}H_{14}$	0.670		
948-67-4	2-Methyl-9,10-dihydroanthracene	$C_{15}H_{14}$	0.752[a]	Combustion	Safarik and Strausz (1997)
203-64-5	4H-Cyclopenta[*def*]phenanthrene	$C_{15}H_{10}$	1.042	Used to produce OLED	Kim et al. (2009)

Table S16. (continued).

CAS#	Compound Name	Formula	Predicted toxicity (EC50, mg L^{-1})	Uses/origins	Reference
575-41-7	1,3-Dimethylnaphthalene	$C_{12}H_{12}$	1.472		
571-58-4	1,4-Dimethylnaphthalene	$C_{12}H_{12}$	1.472		
569-41-5	1,8-Dimethylnaphthalene	$C_{12}H_{12}$	1.472		
644-08-6	4-Methylbiphenyl	$C_{13}H_{12}$	1.485		
92-83-1	9H-Xanthene	$C_{13}H_{10}O$	1.600		
90-12-0	1-Methylnaphthalene	$C_{11}H_{10}$	3.205	Wood combustion	Schauer et al. (2001)
81694-10-2	1,1,1-Trifluoro-3-(1-methyl-2(1H)-quinolinylidene)-2-propanone	$C_{13}H_{10}F_3NO$	-		
140928-46-7	1,4,5,6-Tetramethylbicyclo[*2.2.0*]hexa-2,5-diene-2,3-dicarbonitrile	$C_{12}H_{12}N_2$	-		
74357-40-7	2-(1-methyl-1-propenyl)-(e)-Naphthalene	$C_{14}H_{14}$	-		
125902-73-0	2-(2-furyl)-1,3,4-trimethyl-2,5-dihydrophosphole 1-sulfide	$C_{11}H_{15}OPS$	-		
2000234-55-0	2,3,9-Trimethyl-gamma-carboline	$C_{14}H_{14}N_2$	-		
2000392-49-0	2-Phenyl-3-(2-pyrrolyl)indole	$C_{18}H_{14}N_2$	-		
2000346-27-9	3,4-dihydro-7-methylbenz[*a*]anthracene	$C_{19}H_{16}$	-		
2000305-49-7	6-Methyl-3,4-benzo-beta-carboline	$C_{16}H_{12}N_2$	-		
2000438-54-0	8-Acetyloxy-1-cyano-5-hydroxy-7-methoxy-6-methylisoquinoline	$C_{14}H_{12}N_2O_4$	-		
2000345-65-0	9-(Pyridin-3-yl)-9H-carbazol	$C_{17}H_{12}N_2$	-		
100230-00-0	Benzo[*7,8*]cyclodeca[*1,2,3,4-def*]biphenylene	$C_{22}H_{14}$	-		
2000425-29-6	Dibenzo[*b,kl*]xanthene	$C_{20}H_{12}O$	-		
2000352-95-3	Ethyl 2-Amino-5-(1-methylethyl)indole-3-carboxylate	$C_{14}H_{18}N_2O_2$	-		
2000795-66-8	N-[2-[2-Methyl-1-(p-tolylsulfonyl)propyl]heptanoyl]piperidine	$C_{23}H_{37}NO_3S$	-		
117052-62-7	Pyridazino[1",6":1',2']imidazo[4',5':4,5]imidazo[1,2-b]pyridazine-2,9-diamine	$C_{10}H_8N_8$	-		

Supplementary Figures

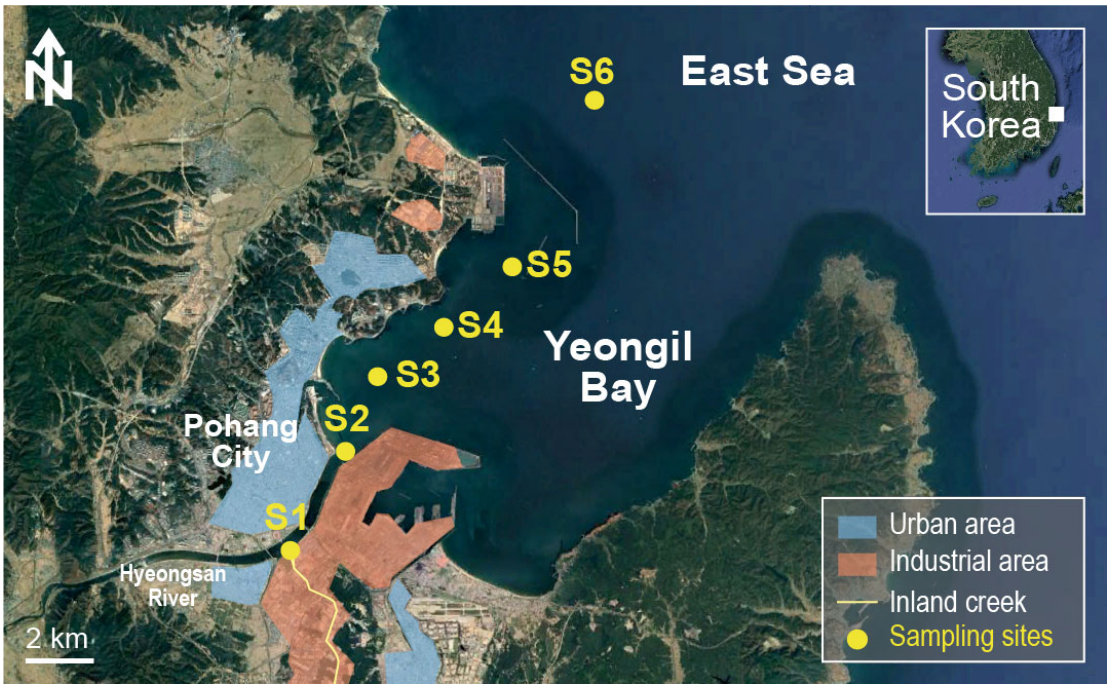

Fig. S1. Map showing sampling sites of sediments in Pohang and Yeongil Bay, South Korea.

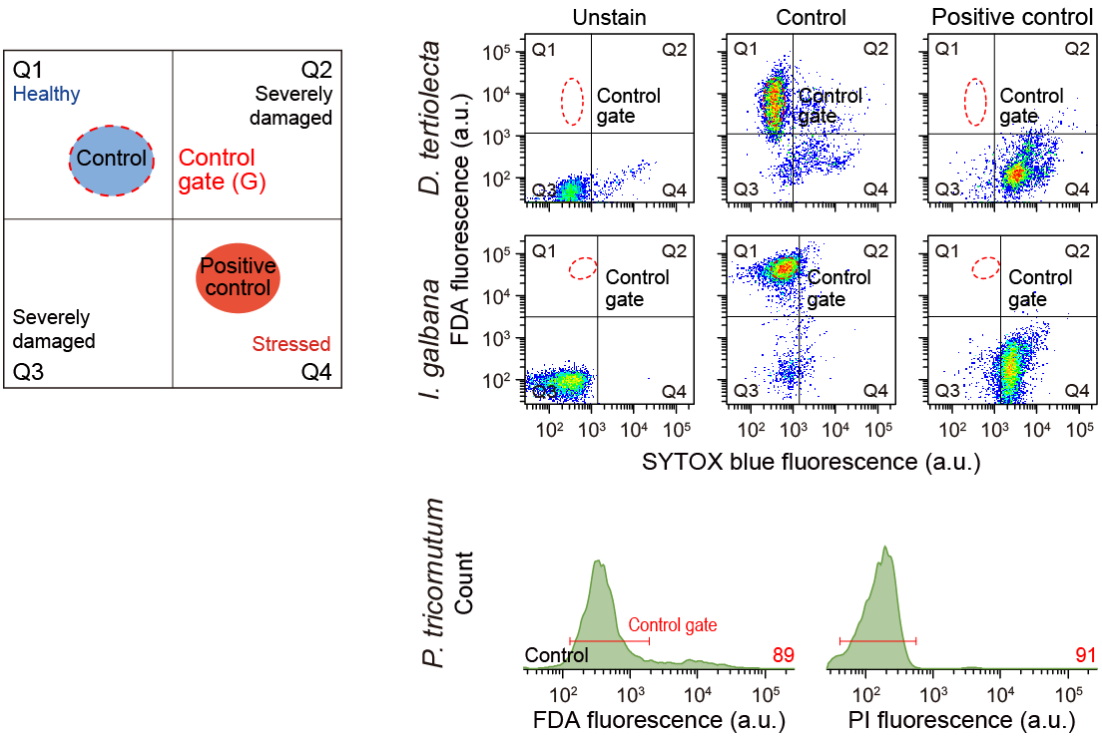

Fig. S2. Bi-dimensional cytograms of the double staining of control cells and control gate of single staining.

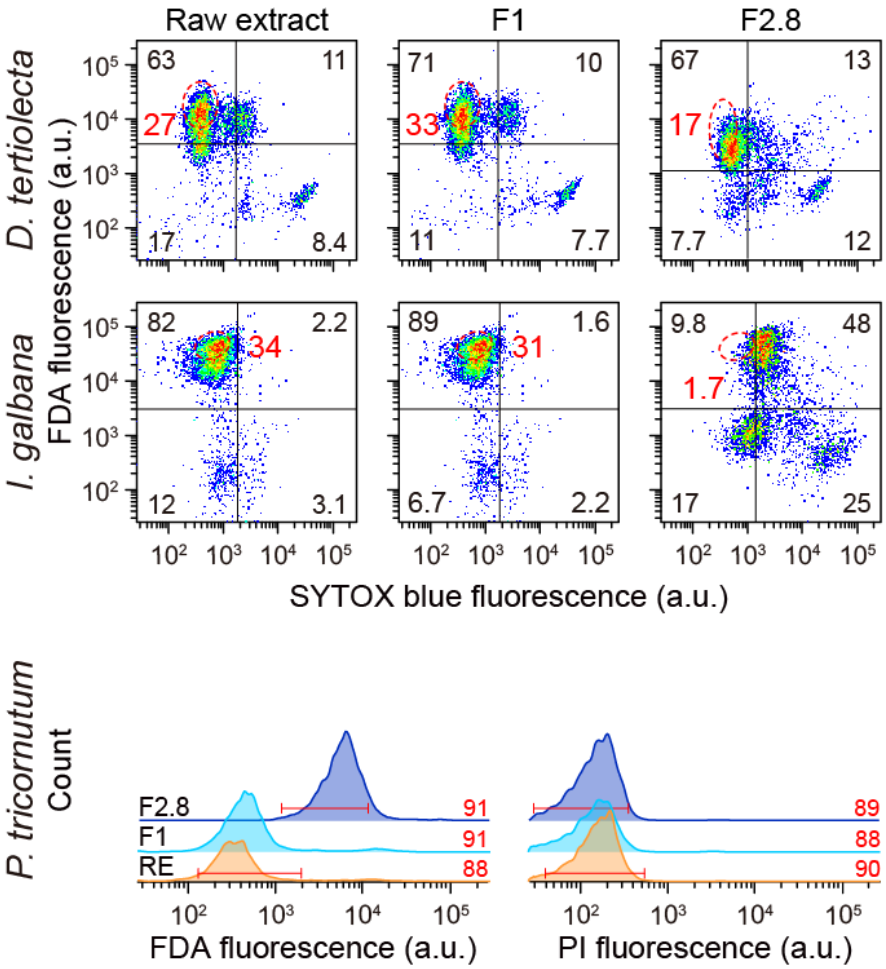

Fig. S3. Results of exposure of the three microalgal species to S1 raw extract, F1, and F2.8.

References

Almeida, A.C., Gomes, T., Habuda-Stanić, M., Lomba, J.A.B., Romić, Ž., Turkalj, J.V., Lillicrap, A., 2019. Characterization of multiple biomarker responses using flow cytometry to improve environmental hazard assessment with the green microalgae *Raphidocelis subcapitata*. Sci. Total Environ. 687, 827–838. https://doi.org/10.1016/j.scitotenv.2019.06.124

Bandow, N., Altenburger, R., Lübcke-von Varel, U., Paschke, A., Streck, G., Brack, W., 2009a. Partitioning-based dosing: An approach to include bioavailability in the effect-directed analysis of contaminated sediment samples. Environ. Sci. Technol. 43, 3891−3896. https://doi.org/10.1021/es803453h

Bandow, N., Altenburger, R., Streck, G., Brack, W., 2009b. Effect-directed analysis of contaminated sediments with partition-based dosing using green algae cell multiplication Inhibition. Environ. Sci. Technol. 43, 7343–7349. https://doi.org/10.1021/es901351z

Benner, B.A., Wise, S.A., Currie, L.A., Klouda, G.A., Klinedinst, D.B., Zweidinger, R.B., Stevens, R.K., Lewis, C.W., 1995. Distinguishing the contributions of residential wood combustion and mobile source emissions using relative concentrations of dimethylphenanthrene isomers. Environ. Sci. Technol. 29, 2382–2389. https://doi.org/10.1021/es00009a034

Booij, P., Vethaak, A.D., Leonards, P.E.G., Sjollema, S.B., Kool, J., de Voogt, P., Lamoree, M.H., 2014. Identification of photosynthesis inhibitors of pelagic marine algae using 96-well plate microfractionation for enhanced throughput in Effect-directed analysis. Environ. Sci. Technol. 48, 8003–8011. https://doi.org/10.1021/es405428t

Cai, H., Liang, J., Ning, X.-a., Lai, X., Li, Y., 2020. Algal toxicity induced by effluents from textile-dyeing wastewater treatment plants. J Environ. Sci. 91, 199−208. https://doi.org/10.1016/j.jes.2020.01.004

CCME, 2002. Canadian sediment quality guidelines for the protection of aquatic life summary table, in: Canadian environmental quailty guidelines, 1999, Canadian Council of Ministers of the Environment Winnipeg., http://ceqgrcqe.ccme.ca/download/en/242?redir=1569847235

Cid, A., Fidalgo, P., Herrero, C., Abalde, J., 1996. Toxic action of copper on the membrane system of a marine diatom measured by flow cytometry. Cytometry 25, 32−36. https://doi.org/10.1002/(sici)1097-0320(19960901)25:1<32::Aid-cyto4>3.0.Co;2-g

Dupraz, V., Ménard, D., Akcha, F., Budzinski, H., Stachowski-Haberkorn, S., 2019. Toxicity of binary mixtures of pesticides to the marine microalgae *Tisochrysis lutea* and *Skeletonema marinoi*: Substance interactions and physiological impacts. Aquat. Toxicol. 211, 148–162. https://doi.org/10.1016/j.aquatox.2019.03.015

Dyremark, A., Westerholm, R., Övervik, E., Gustavsson, J.-Å., 1995. Polycyclic aromatic hydrocarbon (PAH) emissions from charcoal grilling. Atmos. Environ. 29, 1553–1558. https://doi.org/10.1016/1352-2310(94)00357-Q

Egenberg, I.M., Aasen, J.A.B., Holtekjølen, A.K., Lundanes, E., 2002. Characterisation of traditionally kiln produced pine tar by gas chromatography-mass spectrometry. J Anal. Appl. Pyrol. 62, 143–155. https://doi.org/10.1016/S0165-2370(01)00112-7

Esperanza, M., Cid, Á., Herrero, C., Rioboo, C., 2015. Acute effects of a prooxidant herbicide on the microalga *Chlamydomonas reinhardtii*: Screening cytotoxicity and genotoxicity endpoints. Aquat. Toxicol. 165, 210−221. https://doi.org/10.1016/j.aquatox.2015.06.004

Esperanza, M., Seoane, M., Rioboo, C., Herrero, C., Cid, Á., 2019. Differential toxicity of the

UV-filters BP-3 and BP-4 in *Chlamydomonas reinhardtii*: A flow cytometric approach. Sci. Total Environ. 669, 412−420. https://doi.org/10.1016/j.scitotenv.2019.03.116
Franklin, N.M., Stauber, J.L., Lim, R.P., 2001. Development of flow cytometry-based algal bioassays for assessing toxicity of copper in natural waters. Environ. Toxicol. Chem. 20, 160−170. https://doi.org/10.1002/etc.5620200118
Funahashi, M., Hanna, J.-i., 1997. Fast ambipolar carrier transport in smectic phases of phenylnaphthalene liquid crystal. Appl. Phys. Lett. 71, 602–604. https://doi.org/10.1063/1.119806
Gosset, A., Durrieu, C., Barbe, P., Bazin, C., Bayard, R., 2019. Microalgal whole-cell biomarkers as sensitive tools for fast toxicity and pollution monitoring of urban wet weather discharges. Chemosphere 217, 522–533. https://doi.org/10.1016/j.chemosphere.2018.11.033
Grimmer, G., Jacob, J., Naujack, K.W., 1983. Profile of the polycyclic aromatic compounds from crude oils. Fresen. Z Anal. Chemie 314, 29–36. https://doi.org/10.1007/BF00476507
Grote, M., Brack, W., Walter, H.A., Altenburger, R., 2005. Confirmation of cause-effect relationships using effect-directed analysis for complex environmental samples. Environ. Toxicol. Chem. 24, 1420−1427. https://doi.org/10.1897/04-278R.1
Hedberg, E., Kristensson, A., Ohlsson, M., Johansson, C., Johansson, P.-Å., Swietlicki, E., Vesely, V., Wideqvist, U., Westerholm, R., 2002. Chemical and physical characterization of emissions from birch wood combustion in a wood stove. Atmos. Environ. 36, 4823-4837. https://doi.org/10.1016/S1352-2310(02)00417-X
Hong, S., Lee, J., Lee, C., Yoon, S.J., Jeon, S., Kwon, B.-O., Lee, J.-H., Giesy, J.P., Khim, J.S., 2016. Are styrene oligomers in coastal sediments of an industrial area aryl hydrocarbon-receptor agonists? Environ. Pollut. 213, 913–921. https://doi.org/10.1016/j.envpol.2016.03.025
Huang, J., Liu, X., Tang, X., 2000. Study of the anthracene and benzo[*a*]pyrene toxicity effect on marine microalgae. J. Ocean. U. Qingdao 30, 499–502.
Källqvist, T., Milačič, R., Smital, T., Thomas, K.V., Vranes, S., Tollefsen, K.-E., 2008. Chronic toxicity of the Sava River (SE Europe) sediments and river water to the algae *Pseudokirchneriella subcapitata*. Water Res. 42, 2146−2156. https://doi.org/10.1016/j.watres.2007.11.026
Kim, J., Jin, Y., Song, S., Kim, I., Suh, H., 2009. Synthesis of 4H-Cyclopenta[*def*]phenanthrene from 1-Naphthylacetic Acid. Chem. Lett. 38, 1008–1008. https://doi.org/10.1246/cl.2009.1008
Lee, J., Hong, S., Kim, T., Lee, C., An, S.-A., Kwon, B.-O., Lee, S., Moon, H.-B., Giesy, J.P., Khim, J.S., 2020. Multiple bioassays and targeted and nontargeted analyses to characterize potential toxicological effects associated with sediments of Masan Bay: Focusing on AhR-mediated potency. Environ. Sci. Technol. https://doi.org/10.1021/acs.est.9b07390
Liu, W., Chen, S., Quan, X., Jin, Y.-H., 2008. Toxic effect of serial perfluorosulfonic and perfluorocarboxylic acids on the membrane system of a freshwater alga measured by flow cytometry. Environmental toxicology and chemistry 27, 1597− 1604. https://doi.org/10.1897/07-459
Liu, W., Ming, Y., Huang, Z., Li, P., 2012. Impacts of florfenicol on marine diatom *Skeletonema costatum* through photosynthesis inhibition and oxidative damages. Plant Physiol. Bioch. 60, 165−170. https://doi.org/10.1016/j.plaphy.2012.08.009
Machado, M.D., Lopes, A.R., Soares, E.V., 2015. Responses of the alga *Pseudokirchneriella subcapitata* to long-term exposure to metal stress. J Hazard. Meter. 296, 82−92.

https://doi.org/10.1016/j.jhazmat.2015.04.022
Moeris, S., Vanryckeghem, F., Demeestere, K., Huysman, S., Vanhaecke, L., De Schamphelaere, K.A.C., 2019. Growth stimulation effects of environmentally realistic contaminant mixtures on a marine diatom. Environ. Toxicol. Chem. 38, 1313−1322. https://doi.org/10.1002/etc.4431
Niehus, N.C., Floeter, C., Hollert, H., Witt, G., 2018. Miniaturised marine algae test with polycyclic aromatic hydrocarbons − Comparing equilibrium passive dosing and nominal spiking. Aquat. Toxicol. 198, 190–197. https://doi.org/10.1016/j.aquatox.2018.03.002
Nogueira, P.F.M., Nakabayashi, D., Zucolotto, V., 2015. The effects of graphene oxide on green algae *Raphidocelis subcapitata*. Aquat. Toxicol. 166, 29−35. https://doi.org/10.1016/j.aquatox.2015.07.001
Okumura, Y., Koayama, J., Uno, S., 2003. The relationship between $\log P_{ow}$ and molecular weight of polycyclic aromatic hydrocarbons and EC50 values. 41, 182–191.
Olsen, R.O., Hess-Erga, O.K., Larsen, A., Hoffmann, F., Thuestad, G., Hoell, I.A., 2016. Dual staining with CFDA-AM and SYTOX Blue in flow cytometry analysis of UV-irradiated Tetraselmis suecica to evaluate vitality. Aquat. Biol. 25, 39–52. https://doi.org/10.3354/ab00662
Othman, H.B., Leboulanger, C., Le Floc'h, E., Hadj Mabrouk, H., Sakka Hlaili, A., 2012. Toxicity of benz[*a*]anthracene and fluoranthene to marine phytoplankton in culture: Does cell size really matter? J. Hazard. Mater. 243, 204–211. https://doi.org/10.1016/j.jhazmat.2012.10.020
Pikula, K.S., Chernyshev, V.V., Zakharenko, A.M., Chaika, V.V., Waissi, G., Hai, L.H., Hien, T.T., Tsatsakis, A.M., Golokhvast, K.S., 2019. Toxicity assessment of particulate matter emitted from different types of vehicles on marine microalgae. Environ. Res. 179, 108785. https://doi.org/10.1016/j.envres.2019.108785
Prado, R., Rioboo, C., Herrero, C., Cid, Á., 2011. Characterization of cell response in *Chlamydomonas moewusii* cultures exposed to the herbicide paraquat: Induction of chlorosis. Aquat. Toxicol. 102, 10–17. https://doi.org/10.1016/j.aquatox.2010.12.013
Prado, R., Rioboo, C., Herrero, C., Suárez-Bregua, P., Cid, Á., 2012. Flow cytometric analysis to evaluate physiological alterations in herbicide-exposed *Chlamydomonas moewusii* cells. Ecotoxicology 21, 409–420. https://doi.org/10.1007/s10646-011-0801-3
Ramdahl, T., 1983. Retene—a molecular marker of wood combustion in ambient air. Nature 306, 580–582.
Riegraf, C., Reifferscheid, G., Becker, B., Belkin, S., Hollert, H., Feiler, U., Buchinger, S., 2019. Detection and quantification of photosystem II inhibitors using the freshwater alga *Desmodesmus subspicatus* in combination with high-Performance thin-layer chromatography. Environ. Sci. Tech. 53, 13458−13467. https://doi.org/10.1021/acs.est.9b04634
Safarik, I., Strausz, O.P., 1997. The thermal decomposition of hydrocarbons. Part 3. Polycyclic n-alkylaromatic compounds. Res. Chem. Intermediat. 23, 179–195. https://doi.org/10.1163/156856797X00330
Schauer, J.J., Kleeman, M.J., Cass, G.R., Simoneit, B.R.T., 2001. Measurement of emissions from air pollution sources. 3. C_1−C_{29} Organic compounds from fireplace combustion of wood. Environ. Sci. Tech. 35, 1716–1728. https://doi.org/10.1021/es001331e
Schwab, K., Altenburger, R., Varel, U.L.-v., Streck, G., Brack, W., 2009. Effect-directed analysis of sediment-associated algal toxicants at selected hot spots in the River Elbe basin with a

special focus on bioaccessibility. Environ. Toxicol. Chem. 28, 1506–1517. https://doi.org/10.1897/08-340.1

Smital, T., Terzic, S., Zaja, R., Senta, I., Pivcevic, B., Popovic, M., Mikac, I., Tollefsen, K.E., Thomas, K.V., Ahel, M., 2011. Assessment of toxicological profiles of the municipal wastewater effluents using chemical analyses and bioassays. Ecotox. Environ. Saf. 74, 844–851. https://doi.org/10.1016/j.ecoenv.2010.11.010

Tousova, Z., Froment, J., Oswald, P., Slobodník, J., Hilscherova, K., Thomas, K.V., Tollefsen, K.E., Reid, M., Langford, K., Blaha, L., 2018. Identification of algal growth inhibitors in treated waste water using effect-directed analysis based on non-target screening techniques. J. Hazard. Mater. 358, 494–502. https://doi.org/10.1016/j.jhazmat.2018.05.031

Vermeirssen, E.L.M., Hollender, J., Bramaz, N., van der Voet, J., Escher, B.I., 2010. Linking toxicity in algal and bacterial assays with chemical analysis in passive samplers deployed in 21 treated sewage effluents. Environ. Toxicol. Chem. 29, 2575−2582. https://doi.org/10.1002/etc.311

Wang, L., Zheng, B., Meng, W., 2008. Photo-induced toxicity of four polycyclic aromatic hydrocarbons, singly and in combination, to the marine diatom *Phaeodactylum tricornutum*. Ecotox. Environ. Safe. 71, 465–472. https://doi.org/10.1016/j.ecoenv.2007.12.019

Zhao, X.-Y., Zong, Z.-M., Cao, J.-P., Ma, Y.-M., Han, L., Liu, G.-F., Zhao, W., Li, W.-Y., Xie, K.-C., Bai, X.-F., Wei, X.-Y., 2008. Difference in chemical composition of carbon disulfide-extractable fraction between vitrinite and inertinite from Shenfu-Dongsheng and Pingshuo coals. Fuel 87, 565–575. https://doi.org/10.1016/j.fuel.2007.02.021

Zheng, Q., Zhang, Y., Wahyudiono, Fouquet, T., Zeng, X., Kanda, H., Goto, M., 2020. Room-temperature extraction of direct coal liquefaction residue by liquefied dimethyl ether. Fuel 262, 116528. https://doi.org/10.1016/j.fuel.2019.116528.